Mechanisms creating transient and sustained photoresponses in mammalian retinal ganglion cells

Xiwu Zhao,[1] Aaron N. Reifler,[1] Melanie M. Schroeder,[1] Elizabeth R. Jaeckel,[1] Andrew P. Chervenak,[1] and Kwoon Y. Wong[1,2]

[1]Department of Ophthalmology and Visual Sciences and [2]Department of Molecular, Cellular, and Developmental Biology, University of Michigan, Ann Arbor, MI 48105

Retinal neurons use sustained and transient light responses to encode visual stimuli of different frequency ranges, but the underlying mechanisms remain poorly understood. In particular, although earlier studies in retinal ganglion cells (RGCs) proposed seven potential mechanisms, all seven have since been disputed, and it remains unknown whether different RGC types use different mechanisms or how many mechanisms are used by each type. Here, we conduct a comprehensive survey in mice and rats of 12 candidate mechanisms that could conceivably produce tonic rod/cone-driven ON responses in intrinsically photosensitive RGCs (ipRGCs) and transient ON responses in three types of direction-selective RGCs (TRHR+, Hoxd10+ ON, and Hoxd10+ ON-OFF cells). We find that the tonic kinetics of ipRGCs arises from their substantially above-threshold resting potentials, input from sustained ON bipolar cells, absence of amacrine cell inhibition of presynaptic ON bipolar cells, and mGluR7-mediated maintenance of light-evoked glutamatergic input. All three types of direction-selective RGCs receive input from transient ON bipolar cells, and each type uses additional strategies to promote photoresponse transience: presynaptic inhibition and dopaminergic modulation for TRHR+ cells, center/surround antagonism and relatively negative resting potentials for Hoxd10+ ON cells, and presynaptic inhibition for Hoxd10+ ON-OFF cells. We find that the sustained nature of ipRGCs' rod/cone-driven responses depends neither on melanopsin nor on *N*-methyl-D-aspartate (NMDA) receptors, whereas the transience of the direction-selective cells' responses is influenced neither by α-amino-3-hydroxy-5-methyl-4-isoxazolepropionic acid (AMPA)/kainate receptor desensitization nor by glutamate uptake. For all cells, we further rule out spike frequency adaptation and intracellular Ca^{2+} as determinants of photoresponse kinetics. In conclusion, different RGC types use diverse mechanisms to produce sustained or transient light responses. Parenthetically, we find evidence in both mice and rats that the kinetics of light-induced mGluR6 deactivation determines whether an ON bipolar cell responds tonically or transiently to light.

INTRODUCTION

Ever since the earliest intracellular recordings of retinal neurons, four broad varieties of inner retinal light responses have been appreciated: ON versus OFF responses, which signal increments versus decrements in light intensity, and sustained versus transient responses, which transmit versus filter out low stimulus frequencies (Werblin and Dowling, 1969; Kaneko, 1970). Among retinal ganglion cells (RGCs), which are output neurons of the retina, both transient and sustained types have been reported in numerous species, including macaque (Gouras, 1968), mudpuppy (Werblin and Dowling, 1969), cat (Cleland et al., 1971), rabbit (Caldwell and Daw, 1978), tiger salamander (Vallerga and Usai, 1986), frog (Bonaventure et al., 1980), turtle (Granda and Fulbrook, 1989), mouse (Nirenberg and Meister, 1997), tree shrew (Lu and Petry, 2003), rat (Wong et al., 2007), and hamster (Jones et al., 2015).

Because the transient/sustained dichotomy is a fundamental attribute of RGC photoresponses, numerous studies have investigated their origins. Early work suggested seven mechanisms: (1) transient and sustained RGCs have different voltage-gating properties, causing a steady excitatory input to evoke transient spiking in the former but longer-lasting spiking in the latter (Mobbs et al., 1992); (2) transient ON RGCs are downstream from ON bipolar cells that depolarize transiently when metabotropic glutamate receptor 6 (mGluR6) is deactivated in response to light, whereas sustained ON RGCs get input from ON bipolar cells that depolarize tonically upon mGluR6 deactivation (Awatramani and Slaughter, 2000); (3) excitatory bipolar input to RGCs is truncated by delayed presynaptic and/or postsynaptic amacrine cell inhibition to make RGC photoresponses more phasic (Caldwell and Daw, 1978; Bonaventure et

Correspondence to Kwoon Y. Wong: kwoon@umich.edu

Abbreviations used: AMPA, α-amino-3-hydroxy-5-methyl-4-isoxazolepropionic acid; BAPTA, 1,2-bis(2-aminophenoxy)ethane-N,N,N′,N′-tetraacetic acid; CPPG, (RS)-α-cyclopropyl-4-phosphonophenylglycine; GABA, γ-aminobutyric acid; GFP, green fluorescent protein; ipRGC, intrinsically photosensitive RGC; L-AP4, L-(+)-2-amino-4-phosphonobutyric acid; MMPIP, 6-(4-methoxyphenyl)-5-methyl-3-(4-pyridinyl)-isoxazolo[4,5-c]pyridin-4(5H)-one; RGC, retinal ganglion cell; TBOA, DL-threo-β-benzyloxyaspartic acid; TPMPA, (1,2,5,6-tetrahydropyridin-4-yl)methylphosphinic acid; TRHR, thyrotropin-releasing hormone receptor.

The Rockefeller University Press $30.00
J. Gen. Physiol. 2017 Vol. 149 No. 3 335–353
https://doi.org/10.1085/jgp.201611720

al., 1980); (4) dopamine enhances the sustained excitation of some ON RGCs (Jensen and Daw, 1984); (5) α-amino-3-hydroxy-5-methyl-4-isoxazolepropionic acid (AMPA) receptor desensitization increases photoresponse transience (Lukasiewicz et al., 1995); (6) AMPA/kainate receptors trigger faster and more rapidly decaying light responses than NMDA receptors (Ikeda and Sheardown, 1982; Slaughter and Miller, 1983); and (7) glutamate reuptake by transporters produces transient light responses by limiting the duration of RGC activation (Higgs and Lukasiewicz, 1999; Matsui et al., 1999).

However, all of the aforementioned findings have since been challenged. Transient and sustained RGCs were found to produce equally sustained spiking (Sethuramanujam and Slaughter, 2015). Antagonist-induced mGluR6 deactivation excited transient and sustained ON bipolar cells with similar decay rates, which is incompatible with the notion that mGluR6 determines whether a postsynaptic RGC is transient or sustained (Kaur and Nawy, 2012). Dopamine shortened many ON RGCs' light responses (Maguire and Smith, 1985; Vaquero et al., 2001). AMPA/kainate- and NMDA-mediated RGC photoresponses had similar time courses (Diamond and Copenhagen, 1993). Tonic RGCs became phasic upon the blockade of γ-aminobutyric acid (GABA) and/or glycine receptors (Frumkes et al., 1995; Popova et al., 2003). And although blocking AMPA receptor desensitization, glutamate uptake, or inhibition potentiated transient RGC photoresponses, these responses remained essentially transient, with decay rates largely unaffected (Higgs and Lukasiewicz, 1999; Bieda and Copenhagen, 2000). Another limitation is that most studies were done in cold-blooded vertebrates, and it is unclear how many of the results are applicable to mammalian RGCs. Furthermore, most studies sampled from and pooled randomly selected cells, and each paper investigated just one or two mechanisms. Consequently, it remains unknown how many mechanisms are used by each RGC and whether different cell types use different mechanisms. Because there are over 30 physiologically distinct RGC types (Baden et al., 2016), different papers almost certainly sampled from largely nonoverlapping RGC populations. If different RGC types indeed use diverse strategies to create tonic versus transient photoresponses, random sampling could have contributed to the aforementioned disagreements.

Here, we conducted a comprehensive survey to examine these seven mechanisms as well as five previously unexplored mechanisms in several types of mouse ON or ON-OFF RGCs: intrinsically photosensitive RGCs (ipRGCs), which exhibit very tonic full-field light responses, and three types of conventional RGCs, which respond transiently to full-field light (Wong, 2012). All three types of conventional RGCs are direction selective and were chosen because when this project began in 2013, they were the only ON or ON-OFF conventional RGC types to have been genetically labeled with fluorescent proteins. Most importantly, all 12 candidate mechanisms were tested in each cell type so that we could determine how many mechanisms are used by each and whether different RGC types use different mechanisms.

MATERIALS AND METHODS

Animals

All procedures were approved by the Institutional Animal Care and Use Committee at the University of Michigan. This study used Sprague Dawley rats as well as six mouse strains: (1) thyrotropin-releasing hormone receptor (TRHR)–GFP mice with green fluorescent protein (GFP) labeling a type of ON-OFF direction-selective RGC (Rivlin-Etzion et al., 2011); (2) homeobox d10 (Hoxd10)-GFP mice with GFP labeling of ON and ON-OFF direction-selective RGCs that innervate the accessory optic system (Dhande et al., 2013); (3) $Opn4^{Cre/Cre}$ mice ("melanopsin-knockout mice") in which both copies of the melanopsin open reading frame are replaced by the gene encoding Cre recombinase (Ecker et al., 2010); (4) $Opn4^{Cre/+}$; Z/EG mice in which the M1–M5 types of ipRGCs are GFP-labeled (Ecker et al., 2010); (5) $Opn4^{Cre/+}$; fNR1 mice created by crossing $Opn4^{Cre/Cre}$ mice with the floxed NR1 line (Tsien et al., 1996) to knock out the gene for the NR1 subunit of NMDA receptors in ipRGCs; and (6) wild-type mice, which were either wild-type siblings of the above lines or B6129SF2/J mice produced by crossing C57BL/6J with 129S1/SvImJ mice (stock #101045; The Jackson Laboratory). Mice and rats were kept in a 12-h light 12-h dark cycle, with all experiments performed during the light phase. Animals were 2–6 mo old, and both genders were used.

Solutions

Voltage-clamp recordings used an internal solution containing (mM) 120 Cs-methanesulfonate, 3 NaCl, 2 QX314-Cl, 5 tetraethylammonium-Cl, 10 HEPES, 10 1,2-bis(2-aminophenoxy)ethane-N,N,N′,N′-tetraacetic acid (BAPTA)-K_4, 2 Mg-ATP, 0.3 Na-GTP, ∼0.1% Lucifer yellow or ∼0.001% Alexa Fluor 568 hydrazide, and NaOH to set pH at 7.3. In the current-clamp experiment where BAPTA was used to chelate intracellular Ca^{2+}, the internal solution contained (mM) 95 K-gluconate, 10 BAPTA-K_4, 5 NaCl, 4 KCl, 2 EGTA, 10 HEPES, 4 Mg-ATP, 7 $Tris_2$-phosphocreatine, 0.3 Na-GTP, ∼0.001% Alexa Fluor 568 hydrazide, and KOH to set pH at 7.3. All other current-clamp experiments used an internal solution with (mM) 120 K-gluconate, 5 NaCl, 4 KCl, 10 HEPES, 2 EGTA, 4 Mg-ATP, 0.3 Na-GTP, 7 Tris-phosphocreatine, ∼0.1% Lucifer yellow or ∼0.001% Alexa Fluor 568 hydrazide, and KOH to set pH at 7.3.

Unless stated otherwise, the extracellular solution was Ames' medium gassed with 95% O_2 and 5%

Table 1. **Drugs used in this study**

Drug	Action	Concentration	Application method
L-AP4	Activates group III mGluRs	4 or 50 µM	Bath, puffer
BAPTA	Chelates Ca^{2+}	10 mM	Intracellular
Cd^{2+}	Blocks neurotransmitter release	1 mM	Bath
CGP 52432	Blocks $GABA_B$ receptors	5 µM	Bath
Concanavalin A	Blocks desensitization of kainate receptors	300 µg/ml	Bath
CPPG	Blocks group III mGluRs	200 or 600 µM	Bath, puffer
Cyclothiazide	Blocks desensitization of AMPA receptors	60 µM	Bath
Isradipine	Blocks L-type Ca^{2+} channels	10 µM	Bath, puffer
MK-801	Blocks NMDA receptors	1 mM	Intracellular
MMPIP	Blocks mGluR7	10 µM	Bath
NMDA	Activates NMDA receptors	5 mM	Puffer
Picrotoxin	Blocks $GABA_A$ receptors	100 or 200 µM	Bath, puffer
SCH 23390	Blocks D1-class dopamine receptors	60 nM	Bath (2–8 h)
Spiperone	Blocks D2-class dopamine receptors	60 nM	Bath (2–8 h)
Strychnine	Blocks glycine receptors	5 or 10 µM	Bath, puffer
TBOA	Blocks glutamate transporters	25 µM	Bath
TPMPA	Blocks $GABA_C$ receptors	15 or 30 µM	Bath, puffer

CO_2 ("Ames"). Throughout recording, this solution was maintained at 32°C using a temperature controller (Warner Instruments) and fed into the recording chamber at 2–3 ml/min. In the Cd^{2+} experiment shown in Fig. 4 C, the superfusion was switched from a control Ringer containing (mM) 120 NaCl, 3.1 KCl, 1.24 $MgCl_2$, 1 $CaCl_2$, 16 D-glucose, 22.6 $NaHCO_3$, and 0.5 liter glutamine to a solution in which $CaCl_2$ in the control Ringer was replaced with 1 mM $CdCl_2$. In the experiment shown in Fig. 4 E, the retinal slice was superfused by Ames supplemented with 4 µM L-(+)-2-amino-4-phosphonobutyric acid (L-AP4), and a PicoPump (World Precision Instruments) was used to puff Ames containing 4 µM L-AP4 and 600 µM (RS)-α-cyclopropyl-4-phosphonophenylglycine (CPPG) onto the cell being recorded, with the tip of the puffer micropipette positioned 20–30 µm from the soma. (R)-(+)-7-chloro-8-hydroxy-3-methyl-1-phenyl-2,3,4,5-tetrahydro-1H-3-benzazepine hydrochloride (SCH 23390), spiperone, cyclothiazide, and 6-(4-methoxyphenyl)-5-methyl-3-(4-pyridinyl)-isoxazolo[4,5-c]pyridin-4(5H)-one (MMPIP) were dissolved in DMSO, and so in the experiments that used these drugs, the control solution had an equal final concentration of DMSO. In the experiment shown in Fig. 6 C, the retina was superfused by Ames containing 100 µM picrotoxin, 15 µM (1,2,5,6-tetrahydropyridin-4-yl) methylphosphinic acid (TPMPA), 5 µM strychnine, and 10 µM isradipine to block any polysynaptic actions of NMDA, and the puffed solution was Ames containing the same drugs plus 5 mM NMDA. Table 1 lists all drugs used, their actions, concentrations, and routes of application.

Whole-cell recording of mouse ganglion cells

For the experiments using GFP mice, methods were identical to those detailed previously (Zhao et al., 2014), except that in the present study, we used only dorsal retinas. In brief, retinas were isolated from dark-adapted mice under infrared-based night vision devices, cut into quadrants, and a dorsal quadrant flattened on the bottom of a superfusion chamber with the RGC side up. GFP-labeled RGC somas were visualized using an invisible multiphoton laser and whole-cell recorded using a MultiClamp 700B amplifier (Molecular Devices). Superfused retinas were kept in darkness until photostimulation. Light stimuli were MATLAB-controlled, presented from a microdisplay (eMagin SVGA Rev. 2) that had three channels with peak emissions at 439, 515, and 582 nm and delivered to the retina through a 5× objective lens. All stimuli were white light created by activating all three channels, and two kinds of stimuli were tested: a center-selective 200-µm spot comparable with or smaller than the dendritic field diameters of the RGCs being studied (Rivlin-Etzion et al., 2011; Schmidt and Kofuji, 2011; Estevez et al., 2012; Dhande et al., 2013; Hu et al., 2013) and "full-field" light 3 mm in diameter. Intensity calibration of this white light was as previously described (Zhao et al., 2014), and both stimuli were equivalent to 8.8 log quanta cm^{-2} s^{-1} of 515-nm light. After recording, intracellular dye fill was imaged and the five types of ipRGCs distinguished by morphological criteria (Hu et al., 2013).

For the experiments using GFP-less mice (wild-type, $Opn4^{Cre/Cre}$, and $Opn4^{Cre/+}$; fNR1 mice), dark-adapted retinas were prepared as described in the previous paragraph. The ganglion cell layer was visualized through infrared transillumination, and whole-cell recordings made using a MultiClamp 700A or 700B amplifier. Light stimuli were either the abovementioned center-selective white spot presented via the objective lens or full-field 8.5 log quanta cm^{-2} s^{-1} 480-nm light presented from below the transparent bottom of the superfusion chamber. We recorded from M4 ipRGCs by targeting the largest somas, and their identity was confirmed by

their α-like dendritic morphology (Ecker et al., 2010) and sustained ON light responses (Zhao et al., 2014). In the experiment shown in Fig. 6 C (top), we found conventional RGCs by recording from randomly selected large somas in the ganglion cell layer and looking for those giving transient ON or OFF responses to 10-s full-field light steps.

In most experiments, each cell's light responses were recorded before and during the application of certain drugs, which often changed the resting potential in current-clamp experiments. This change could confound interpretation of the results by altering ionic driving forces. Thus, after adding the drugs, we used current injection to keep the resting potential at the predrug level.

Whole-cell recording of mouse and rat bipolar cells

Under dim red light, dark-adapted animals were euthanized using CO_2 followed by cervical dislocation. Eyes were enucleated, hemisected, and put into Ames at room temperature. The sclera was removed and the retinas halved. Each half was flattened on a 0.45-µm HA filter paper (EMD Millipore), with the vitreal side down, and cut into 400 µm-thick slices using Feather blades (Ted Pella) mounted on a manual tissue slicer (Stoelting). Slices were kept in darkness in Ames at room temperature for up to 8 h before being used for whole-cell recording. A single slice was mounted with the paper strip perpendicular to the surface of the recording chamber, and superfused with 32°C Ames at 2–3 ml/min. The superfused slice was kept in darkness until stimulus presentation. With the slice visualized through infrared transillumination, a glass micropipette with 5–10-µm tip diameter was placed near the surface of the inner nuclear layer and gentle suction applied to remove the top three or four layers of cells and debris in a small area, exposing deeper bipolar cell somas. Whole-cell current-clamp recordings were made from randomly selected bipolar cells using a MultiClamp 700A amplifier and recording micropipettes with 10–15-MΩ tip resistances. Full-field 480-nm light was presented from below the recording chamber, with an intensity of ~9 log quanta cm^{-1} s^{-1}.

Data analysis

In the figures showing averaged current-clamp recordings, the raw recordings were low-pass-filtered at 10 Hz to filter out action potentials before averaging. To quantify the sustainedness of an ON photoresponse, response amplitude relative to the baseline was measured at the peak of the response and near the end of the stimulus, and the latter was divided by the former to compute the "final-to-peak ratio." To quantify the sustainedness of a current- or light-induced spiking response, the final-to-peak ratio was calculated by dividing the number of current- or light-evoked spikes during the 10th second by that during the 1st second. The more sustained a response was, the higher its final-to-peak ratio would be. A negative ratio indicates that near the end of the stimulus, the voltage, current, or spike rate was below the prestimulus level. Note that this method would not detect relatively small changes in sustainedness, e.g., an increase in photoresponse duration from 3 s to 5 s upon drug application. Thus, throughout this study, we only probed for treatments having more dramatic impacts on photoresponse kinetics. We chose not to calculate time constants because in most cases the photoresponse decay could not be well fit by a single or double exponential decay.

In Fig. 5 C (bottom), the peak amplitude of each RGC's amacrine-driven ON photocurrent (Fig. 5 C, top) was multiplied by the corresponding RGC type's averaged membrane resistance, calculated using Ohm's law ($R = \Delta V/\Delta I$) from responses in the current-injection experiment shown in Fig. 3 A (top).

To assess whether two datasets were significantly different, normally distributed data were compared using the Student *t* test, whereas nonnormal data were compared using the Mann–Whitney *U* test. Significance level was set at $P = 0.05$. Error values are SEM, which are shown in most figures as one-sided error bars to reduce clutter. In the experiments that did not measure light responses (Figs. 3 A and 4 F), the data from the two types of Hoxd10+ RGCs were pooled.

RESULTS

We had previously shown that among rodent RGCs, only ipRGCs could respond continuously to 10-s full-field light steps, whereas all conventional ON or ON-OFF RGCs responded for no more than several seconds (Wong, 2012). In the present study, we again used 10-s stimuli and tested whether any of the hypothesized mechanisms could prolong the response of a conventional RGC to the full stimulus duration and whether any of them would impact an ipRGC's ability to signal 10 s of steady light.

We investigated the rod/cone-driven ON photoresponses of TRHR-expressing RGCs (Rivlin-Etzion et al., 2011), Hoxd10-expressing ON RGCs, Hoxd10+ ON-OFF RGCs (Dhande et al., 2013), and the five types (M1–M5) of ipRGCs. The ON responses of the three types of conventional RGCs are mediated by the ON channel because they could be abolished by L-AP4, which blocks the light response of ON bipolar cells (Fig. 1). Although ipRGCs generate intrinsic, melanopsin-based light responses as well as rod/cone-mediated responses, all stimuli in the current study were at least one log unit below the melanopsin threshold intensity (Zhao et al., 2014), allowing us to selectively examine rod/cone-mediated light responses triggered mainly through the ON channel (Wong et al., 2007). Unless stated otherwise, data from the five ipRGC types were

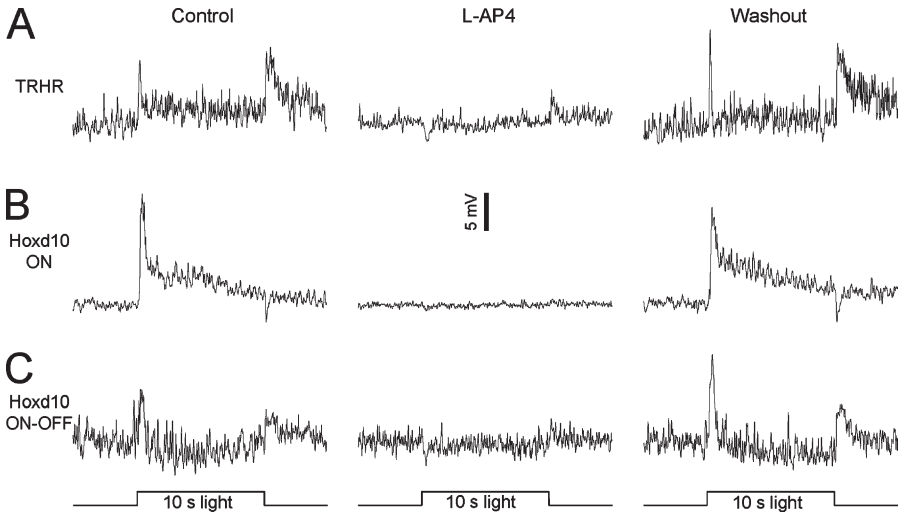

Figure 1. **The ON light responses of the three types of GFP-labeled conventional RGCs are driven by the ON channel.** (A–C) The ON light responses of TRHR+ cells (A), Hoxd10+ ON cells (B), and Hoxd10+ ON-OFF cells (C) were eliminated in the presence of 50 µM L-AP4, an ON channel blocker (second column). Stimuli were the center-selective white light spot. All recording traces were low-pass filtered offline at 10 Hz to remove action potentials.

pooled, which can be justified by our previous demonstration that all five types' rod/cone-mediated light responses are equally sustained (Zhao et al., 2014).

Receptive field surround antagonism

The receptive fields of bipolar cells and downstream neurons consist of center and surround regions that, when illuminated, trigger voltage changes of opposite polarities. Because the surround input involves more synapses than the center input, surround-mediated light responses may be delayed relative to center-mediated ones (Werblin and Dowling, 1969). We hypothesized that the surround response develops gradually in some conventional RGCs and hence makes their ON light responses more transient: the faster center input first evokes a depolarization, which then gets progressively smaller when the slower surround input induces a hyperpolarization. We tested this hypothesis by presenting each RGC with a center-selective light spot and an equal-intensity full-field light, both 10 s in duration. If the hypothesis is correct, the full-field light should evoke a more transient depolarization than the center-selective spot, producing a lower final-to-peak ratio (see Materials and methods) than the center spot.

The full-field light evoked very tonic responses in ipRGCs with a final-to-peak ratio of 0.48 ± 0.06, but in the conventional RGCs, it evoked responses that fully decayed to baseline within several seconds, with final-to-peak ratios that were statistically indistinguishable from zero: −0.05 ± 0.06 for TRHR+ cells, −0.16 ± 0.08 for Hoxd10+ ON cells, and −0.02 ± 0.02 for Hoxd10+ ON-OFF cells (Fig. 2 A). The center spot induced significantly larger ($P < 0.05$) ON responses in M2-M5 ipRGCs, TRHR+ cells, and Hoxd10+ ON cells, confirming center/surround antagonism in the ON input to these cells (Fig. 2 A). In contrast, the two stimuli evoked similarly sized ($P > 0.05$) ON responses in Hoxd10 ON-OFF cells (Fig. 2 A) and M1 ipRGCs. In ipRGCs, TRHR+ cells, and Hoxd10+ ON-OFF cells, the full-field and center-selective stimuli induced responses with statistically similar final-to-peak ratios (Fig. 2 B). Because M1 ipRGCs lack surround inhibition, we also analyzed M2–M5 ipRGCs separately, but we still saw no significant differences in the final-to-peak ratio between full-field and center responses. In contrast, Hoxd10+ ON cells' responses to the center spot lasted throughout the 10-s light step (Fig. 2 A), producing a significantly higher final-to-peak ratio (0.22 ± 0.05) than that of their full-field responses (Fig. 2 B), suggesting that the hypothesized mechanism applies to this cell type.

For consistency, all experiments described below used the center spot unless stated otherwise.

Intrinsic mechanisms: spike rate adaptation, resting potential, intracellular Ca^{2+}, and melanopsin

In the next set of experiments, we asked whether four properties intrinsic to the RGCs might shape their photoresponse kinetics. The first experiment examined whether the various RGC groups possess different voltage-gating properties such that in response to steady current injection, ipRGCs would generate sustained spiking, whereas the conventional RGCs would spike more transiently. For each cell, we held it at its resting potential and injected a 10 s current step of an amplitude that induced the same peak depolarization as the abovementioned center-selective light spot, to learn whether a difference in spiking behavior could explain the kinetics difference in the cell types' responses to this light. All cells spiked throughout the 10-s injection (Fig. 3 A, top). To quantify how sustained the responses were, we divided the number of current-induced spikes during the 10th second of injection by that during the first second, and found this ratio to be statistically indistinguishable among the RGC groups (Fig. 3 A, bottom), thereby refuting the hypothesis that differences in spiking behavior affect the sustainedness of the light responses.

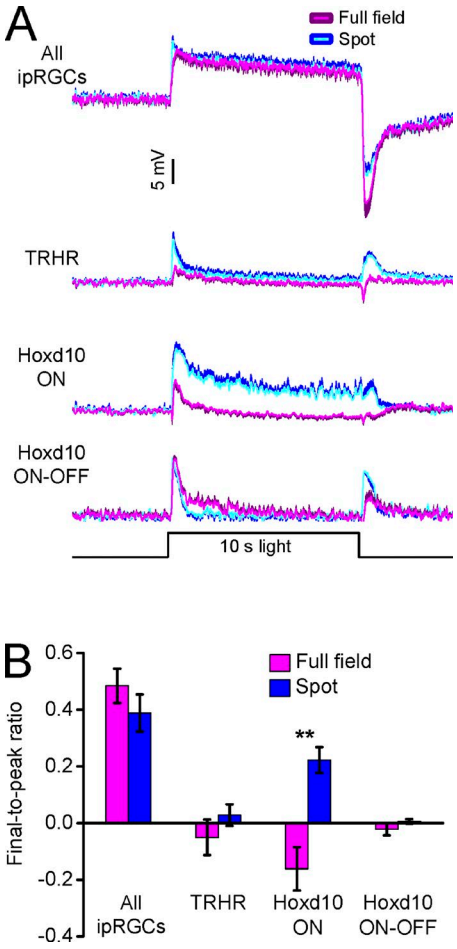

Figure 2. **Suppression by the receptive field surround makes Hoxd10+ ON cells more transient.** (A) Averaged responses of the four RGC groups to full-field (magenta traces) versus center-selective (blue traces) white light steps, with the darkened areas above or below the lighter traces representing SEM. (B) Final-to-peak ratios of the ON light responses shown in A. *n* values: ipRGCs = 12 cells; TRHR+ RGCs = 11 cells; Hoxd10+ ON RGCs = 7 cells; Hoxd10+ ON-OFF RGCs = 7 cells. Error values are SEM. **, $P < 0.01$.

The second experiment examined whether the kinetics of an RGC's spiking response to light is influenced by its resting potential. We previously found all ipRGCs to be unusually depolarized at rest and to spike spontaneously at very high rates (Zhao et al., 2014; Reifler et al., 2015), prompting us to hypothesize that this constitutive depolarization helps generate tonic spiking during prolonged illumination by keeping the cell significantly above the spike threshold. ipRGCs in the present study had, on average, a resting potential of −54.1 ± 2.8 mV and a basal firing rate of 37.7 ± 10.6 Hz. In contrast, the conventional RGCs had substantially more negative resting potentials and lower basal firing rates: −62.2 ± 11.6 mV and 6.5 ± 1.4 Hz for TRHR+ cells, −66.1 ± 2.3 mV and 0.0 ± 0.0 Hz for Hoxd10+ ON cells, and −71.4 ± 1.9 mV and 1.1 ± 0.7 Hz for Hoxd10+ ON-OFF cells. Thus, we hypothesized that for some conventional RGCs, a prolonged light might depolarize the cell above the spike threshold only initially, resulting in a more transient spiking response. To test this possibility, we injected negative currents to make ipRGCs about as hyperpolarized as the conventional RGCs and positive currents to make conventional RGCs roughly as depolarized as ipRGCs. During current injection, basal spike rates were 16.3 ± 8.2 Hz for ipRGCs, 16.4 ± 2.5 Hz for TRHR+ RGCs, 1.3 ± 0.9 Hz for Hoxd10+ ON RGCs, and 13.1 ± 2.8 Hz for Hoxd10+ ON-OFF RGCs. Under both voltage levels, a 10-s-duration center spot was presented, and the sustainedness of the spiking response quantified using the final-to-peak ratio. We found that artificially hyperpolarizing ipRGCs indeed made their light-evoked spiking responses significantly more transient and depolarizing Hoxd10+ ON cells rendered them more tonic (Fig. 3 B, top), whereas the final-to-peak ratio was statistically unchanged for TRHR+ and Hoxd10+ ON-OFF cells (Fig. 3 B, bottom). Thus, the hypothesized mechanism affects only ipRGCs and Hoxd10+ ON cells.

The third experiment tested whether intracellular Ca^{2+} might modulate the kinetics of an RGC's light response, a hypothesis inspired by the observation that intracellular Ca^{2+} made mouse rod bipolar cells more transient (Berntson et al., 2004). We tested this possibility by comparing RGC light responses recorded using the normal K^+-based internal solution versus those recorded using an internal solution containing the Ca^{2+} chelator BAPTA. In both cases, photoresponses were recorded at least 10 min after establishing whole-cell recording. Though the light responses of ipRGCs and Hoxd10+ ON cells became larger (Fig. 3 C, top), the final-to-peak ratios of all cell types' light responses were not significantly affected by BAPTA (Fig. 3 C, bottom), thereby refuting the hypothesis that intracellular Ca^{2+} modulates light response kinetics in RGCs.

In the fourth experiment, we tested the possibility that melanopsin might make the rod/cone-mediated light response of ipRGCs more sustained. The presence of melanopsin is the defining feature distinguishing ipRGCs from all conventional RGCs, and because this photopigment is G protein coupled, it could conceivably modulate the kinetics of synaptic input through G-protein signaling. To test this hypothesis, we compared the rod/cone-driven light responses of wild-type versus melanopsin-knockout ipRGCs. Because our melanopsin-knockout mice lacked GFP labeling, we performed this experiment only on M4-type ipRGCs, which can be readily identified by their large somas (Ecker et al., 2010). This knockout line had a mixed BL/6;129SvJ background (Ecker et al., 2010), and so we used wild-type controls of a similar background (see Materials and methods). We tested full-field light instead of the 200-µm spot because melanopsin is coex-

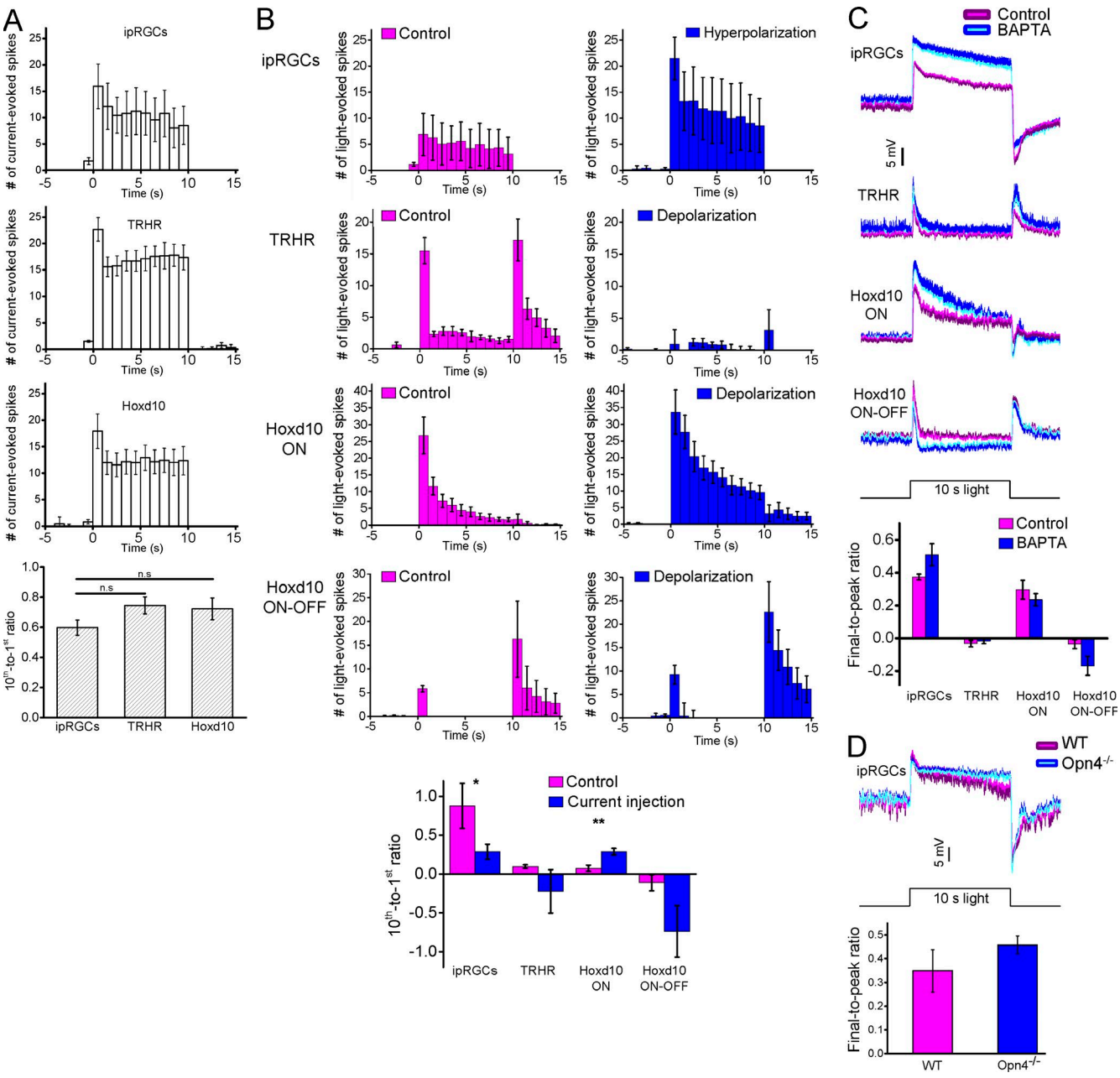

Figure 3. **Examining the dependence of RGC photoresponse kinetics on intrinsic properties.** (A) All RGC groups exhibited equally sustained spiking responses to injected current. Most cells showed spontaneous spiking, which was normalized to zero in these histograms. (top) 1-s-bin histograms of the three RGC groups' spiking responses to current steps injected from 0 to 10 s. (bottom) Ratios of the current-evoked spike count in the 10th second to that during the 1st second. *n* values: ipRGCs = 8; TRHR = 7; Hoxd10 = 9. (B) The resting potential influences the kinetics of ipRGCs' and Hox10+ ON RGCs' spiking responses to light. Most cells had spontaneous spiking, which was normalized to zero in all histograms. (top) Light-induced spiking responses were recorded when the four RGC groups were at their normal resting potentials (magenta plots) or when currents were injected to hyperpolarize ipRGCs and to depolarize the conventional RGCs (blue plots). Center-selective light steps were given from 0 to 10 s. (bottom) Ratios of the 10th-second light-induced spike count to the 1st-second light-induced spike count. Some ratios were negative because spikes rates near the end of the stimulus were below prestimulus levels. *n* values: ipRGCs = 8; TRHR = 6; Hoxd10 ON = 6; Hoxd10 ON-OFF = 5. *, $P < 0.05$; **, $P < 0.01$. (C) Chelating intracellular Ca^{2+} did not significantly alter light response kinetics. (top) Averaged center spot-evoked responses recorded without intracellular BAPTA (magenta recordings) and with intracellular BAPTA (blue recordings). (bottom) Final-to-peak photoresponse ratios. *n* values for recordings without BAPTA: ipRGCs = 16; TRHR = 7; Hoxd10 ON = 8; Hoxd10 ON-OFF = 8. *n* values for recordings with BAPTA: ipRGCs = 14; TRHR = 8; Hoxd10 ON = 5; Hoxd10 ON-OFF = 5. (D) Melanopsin does not make ipRGCs' rod/cone-mediated light responses more tonic. (top) Averaged light responses in wild-type versus melanopsin-knockout ipRGCs. The stimulus was full-field 480-nm light. (bottom) Final-to-peak photoresponse ratios. *n* values: wild-type ipRGCs = 7; melanopsin-knockout ipRGCs = 13. Error values are SEM.

tensive with an ipRGC's entire dendritic field (Wong et al., 2007) and thus its modulation of synaptic input could occur in distal dendrites. Melanopsin-knockout and control mice gave equally sustained light responses (Fig. 3 D), indicating that melanopsin does not make M4 ipRGCs' rod/cone-driven light responses more tonic.

Selective input from sustained versus transient ON bipolar cells

Rods and cones release glutamate in darkness, and glutamate activates mGluR6 on postsynaptic ON bipolar cells to close cation channels and hence cause hyperpolarization. Light suppresses glutamate release and the resultant mGluR6 deactivation allows cation channels to open, causing depolarization (Dowling and Ripps, 1973; Slaughter and Miller, 1981; Copenhagen and Jahr, 1989; Masu et al., 1995). Awatramani and Slaughter (2000) tested the hypothesis that the kinetics difference between tonic and transient ON bipolar cells' light responses is caused by their different mGluR6 deactivation kinetics. They bath-applied the mGluR antagonist CPPG to mimic a light stimulus whose intensity rises slowly before reaching steady state and observed that each cell's CPPG-induced depolarization had roughly the same amplitude as its steady-state photoresponse (i.e., ON bipolars with tonic light responses depolarized more than those with transient light responses), leading them to conclude that the sustained/transient dichotomy in ON bipolar photoresponses arises from a diversity in mGluR6 deactivation kinetics. CPPG likewise depolarized sustained ON RGCs more than transient ones, suggesting that sustained RGCs receive input from sustained bipolar cells, whereas transient RGCs get transient bipolar input (Awatramani and Slaughter, 2000). However, this conclusion was challenged by a subsequent study reporting that putative sustained and transient ON bipolar cells responded to mGluR antagonists with comparable kinetics (Kaur and Nawy, 2012). This controversy, along with the fact that both papers studied only salamanders, prompted us to repeat these experiments in mice.

When we measured bipolar-mediated, center-selective light responses by voltage-clamping RGCs at E_{Cl} to nullify amacrine-driven Cl^- currents, we found these responses to be more sustained in ipRGCs than in the conventional RGCs (Fig. 4 A). But this could be caused by factors other than a difference in mGluR6 deactivation; for example, the ON bipolar cells presynaptic to conventional RGCs could receive stronger amacrine cell feedback than those feeding ipRGCs, and this feedback truncates the ON bipolar cells' glutamate release. The next set of experiments tested the hypothesis of Awatramani and Slaughter (2000) that mGluR6 deactivation kinetics determines an ON bipolar cell's photoresponse kinetics, which in turn defines the postsynaptic RGC's photoresponse kinetics. We began by bath-applying CPPG onto several ON bipolar cells whose light responses exhibited a wide range of final-to-peak ratios, and we observed the same trend reported by Awatramani and Slaughter (2000), i.e., the amplitude of CPPG-induced depolarization was directly correlated to photoresponse sustainedness (Fig. 4 B). But Awatramani and Slaughter (2000) noted a caveat of this result: bath-applied CPPG depolarizes not only ON bipolar cells but also postsynaptic amacrine cells, and it is conceivable that the amacrines provide stronger inhibitory input to transient ON bipolar cells than to sustained ones, thus reducing transient bipolar cells' CPPG responses. To circumvent this caveat, Awatramani and Slaughter (2000) deactivated mGluR6 by applying Cd^{2+} instead of CPPG to block transmitter release at all synapses, including those between amacrine and bipolar cells. We did the same and again saw a correlation between ON bipolar photoresponse sustainedness and the Cd^{2+}-induced depolarization (Fig. 4 C). These results validated the hypothesis that mGluR6 deactivation kinetics governs an ON bipolar cell's photoresponse time course. We wondered whether there might be differences among rodent species, so we repeated the CPPG experiment in rat ON bipolar cells and observed the same correlation between CPPG- and light-induced responses (Fig. 4 D).

However, it is conceivable that our results agreed with Awatramani and Slaughter (2000) merely because we repeated their experiments rather than those of Kaur and Nawy (2012). It was important to also repeat the key experiment of Kaur and Nawy (2012) because they tested responses to mGluR antagonists under different conditions: they first applied L-AP4 to activate mGluR6 and then rapidly applied an antagonist to deactivate mGluR6. L-AP4 might activate mGluR6 differently from endogenous glutamate, and the rapid antagonist application mimicked responses to light steps rather than steady-state photoresponses so that mGluR6 deactivation kinetics could be measured directly. Thus, we recorded from rat ON bipolar cells with L-AP4 already in the bath to activate mGluR6 and puffed CPPG to rapidly deactivate mGluR6. We found the final-to-peak ratios of the CPPG responses to be directly correlated with those of the light-step responses (Fig. 4 E).

In the last of this set of experiments, we bath-applied CPPG while recording from mouse ipRGCs, TRHR+ RGCs, and Hoxd10+ RGCs. CPPG depolarized ipRGCs significantly more than the conventional RGCs (Fig. 4 F), corroborating the conclusion of Awatramani and Slaughter (2000) that sustained and transient RGCs receive input from sustained and transient bipolar cells, respectively.

Regulation by amacrine cells

Amacrine cells can regulate the light responses of RGCs by releasing the fast-acting inhibitory transmit-

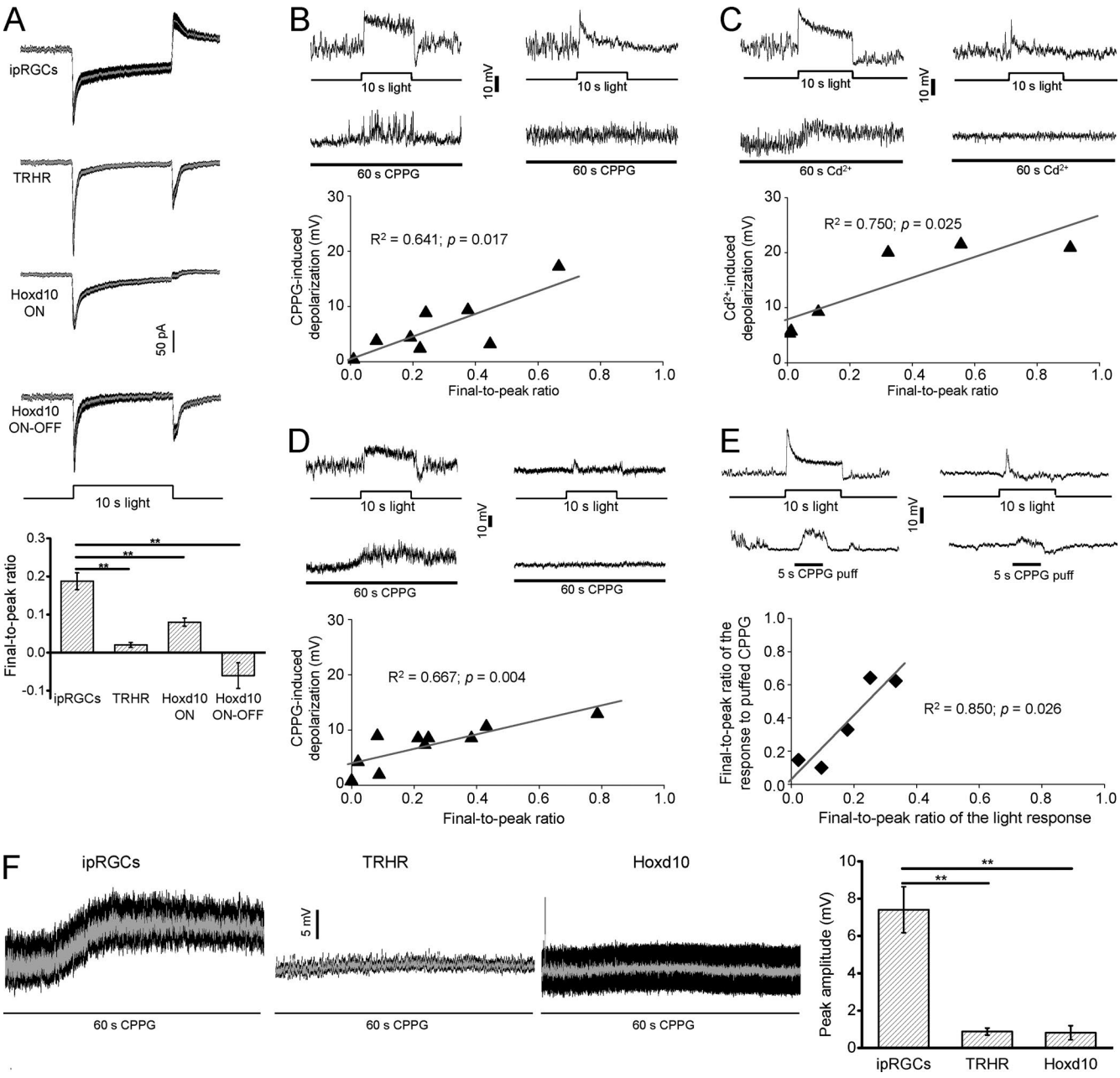

Figure 4. **Selective input from tonic versus phasic ON bipolar cells.** (A) ON bipolar cell–mediated light responses were more tonic in ipRGCs than in conventional RGCs. Voltage-clamp recordings were made at E_{Cl} to isolate cationic, bipolar-driven input. (top) Averaged recordings. The stimulus was the center spot. (bottom) Final-to-peak photoresponse ratios. *n* values: ipRGCs = 25; TRHR = 12; Hoxd10 ON = 11; Hoxd10 ON-OFF = 12. (B) The amplitude of CPPG-induced depolarization in ON bipolar cells was correlated with the sustainedness of light-evoked depolarization. (top left) The response of a sustained ON bipolar cell to full-field 480-nm light measured during superfusion with normal Ames (top recording) and the same cell's subsequent response to 200 µM CPPG bath-applied in darkness (bottom recording). (top right) A transient ON bipolar cell's responses to the same full-field 480-nm light (top recording) and to bath-applied CPPG (bottom recording). (bottom) Analysis of the results from all cells. The linear fit shows a direct correlation between the CPPG-induced depolarization and the final-to-peak ratio of the photoresponse. (C) Cd^{2+} had similar effects to CPPG. Panels in C are identical to panels in B except that 1 mM Cd^{2+} instead of CPPG was bath-applied. (D) The correlation between CPPG-induced depolarization and photoresponse sustainedness was also seen for rat ON bipolar cells. Panels in D are identical to panels in B except for the species difference. (E) In rat ON bipolar cells, mGluR6 deactivation kinetics and photoresponse kinetics were correlated. (top left) A sustained cell's responses to full-field 480 nm light (top recording) and to 600 µM CPPG puffed in the presence of L-AP4 (bottom recording). (top right) A transient cell's responses to light (top recording) and to CPPG puffed in the presence of L-AP4 (bottom recording). (bottom) The final-to-peak ratios of the responses to puffed CPPG and to light. (F) CPPG depolarized ipRGCs significantly more than conventional RGCs. (left) Averaged current-clamp recordings. (right) Averaged peak amplitudes of CPPG-induced depolarization. *n* values: ipRGCs = 14; TRHR = 6; Hoxd10 = 10. Error values are SEM. **, P < 0.01.

ters GABA and glycine or a variety of neuromodulators that exert slower but longer-lasting effects (Brecha, 2004; Masland, 2012). As mentioned in the Introduction, previous studies have investigated regulation of RGC photoresponses by GABA/glycine signaling and by dopamine, a key retinal neuromodulator (Witkovsky, 2004). The experiments in this section showed that both mechanisms shape photoresponse kinetics in mouse RGCs.

Amacrine cells release GABA and glycine onto RGCs to activate an inhibitory Cl^- conductance (postsynaptic inhibition) or onto bipolar cells to suppress glutamate release and consequent activation of excitatory cationic conductances in RGCs (presynaptic inhibition; Zhang and McCall, 2012). We started by assessing the overall impact of GABA and glycine on RGC light responses by recording under current clamp so that both forms of inhibition were detectable. 10-s center spots were first presented while retinas were superfused with normal Ames and again after the addition of antagonists for $GABA_A$, $GABA_B$, $GABA_C$, and glycine receptors. These drugs made all RGCs' light responses larger (Fig. 5 A, top) and more sustained, although their impact on the conventional RGCs' final-to-peak ratios appeared more substantial than on ipRGCs'. In fact, in these drugs, Hoxd10+ ON cells were even more sustained than ipRGCs in normal Ames (Fig. 5 A, bottom). We then asked whether the antagonist-induced increase in sustainedness arose in part from blocking amacrine cell inhibition of presynaptic ON bipolar cells. To answer this, we isolated cationic bipolar cell input by voltage-clamping the RGCs at E_{Cl} so that postsynaptic Cl^- currents were nullified, and we presented the same light spot during superfusion by normal Ames and then in the presence of GABA/glycine antagonists. Though the drugs made the bipolar-driven light responses of all three types of conventional RGCs larger (Fig. 5 B, top), suggesting these RGCs' presynaptic ON bipolar cells received amacrine inhibition, only the responses of TRHR+ cells and Hoxd10+ ON-OFF cells became significantly more tonic (Fig. 5 B, bottom). In contrast, the drugs had little to no effect on ipRGCs' bipolar-driven light responses (Fig. 5 B, top).

Because the sustainedness of all RGCs' light responses seemed to increase more in the current-clamp recordings detecting presynaptic plus postsynaptic inhibitions (Fig. 5 A, bottom) than in the voltage-clamp recordings measuring just presynaptic inhibition (Fig. 5 B, bottom), postsynaptic inhibition likely enhances the photoresponse transience of all four RGC groups. To probe for the presence of postsynaptic inhibition, voltage-clamp recordings were made at $E_{cations}$ to nullify cationic bipolar cell input and isolate amacrine-induced Cl^- conductances, and revealed that all RGCs had sizeable amacrine-driven light responses (Fig. 5 C, top). These amacrine-driven responses of the four RGC groups had comparable kinetics, with statistically similar final-to-peak ratios (Fig. 5 C, middle top) and times to peak (Fig. 5 C, middle bottom). But they were smaller in ipRGCs than in the other RGCs (Fig. 5 C, top), and their estimated impacts on membrane potential were smaller in ipRGCs than in TRHR+ and Hoxd10+ ON-OFF cells (Fig. 5 C, bottom).

To assay for dopaminergic modulation of photoresponse kinetics, we used SCH 23390 and spiperone to antagonize endogenous activation of D1- and D2-class dopamine receptors. Because dopamine induces long-term effects that can take a long time to reverse (Witkovsky, 2004), we did not acutely apply dopamine antagonists in the manner we applied GABA/glycine antagonists. Instead, we recorded light responses from RGCs that had been incubated in the dopamine antagonists for 2–8 h and compared them with those recorded on separate days from RGCs that had been incubated for 2–8 h in Ames containing just the carrier solvent, DMSO; both sets of experiments were conducted during the light phase of the light/dark cycle. Results showed that antagonizing dopamine receptors caused TRHR+ cells' light responses to become significantly more tonic (Fig. 5 D) without significantly changing resting potentials. Although ipRGCs' and Hoxd10+ ON-OFF cells' photoresponses also seemed altered (Fig. 5 D, top), the final-to-peak ratios were not significantly affected (Fig. 5 D, bottom).

AMPA/kainate receptor desensitization and NMDA receptors

As mentioned earlier, previous work suggested that the desensitization of AMPA receptors helps create transient photoresponses in RGCs, leading us to hypothesize that such desensitization likewise contributes to the transience of conventional RGCs, whereas the AMPA receptors on ipRGCs might evade desensitization, as has been demonstrated for OFF bipolar cells (Pang et al., 2008). We tested this by using cyclothiazide to block the desensitization of AMPA receptors. In case glutamatergic input to mouse RGCs also involves kainate receptors, concanavalin A was coapplied to block kainate receptor desensitization. However, because desensitizing AMPA/kainate receptors are present on amacrine cells as well as RGCs (Maguire, 1999; Tran et al., 1999), applying cyclothiazide and concanavalin A alone would impact not only AMPA/kainate receptors on RGCs but also those on amacrine cells, thereby altering amacrine input to RGCs. Thus, we first blocked amacrine signaling using the abovementioned GABA/glycine antagonists and then added the desensitization blockers. Blocking AMPA/kainate desensitization in this manner affected the conventional RGCs' light responses only slightly (Fig. 6 A, top), and their final-to-peak ratios were not significantly altered (Fig. 6 A, bottom). Unexpectedly, ipRGC photoresponses became substantially

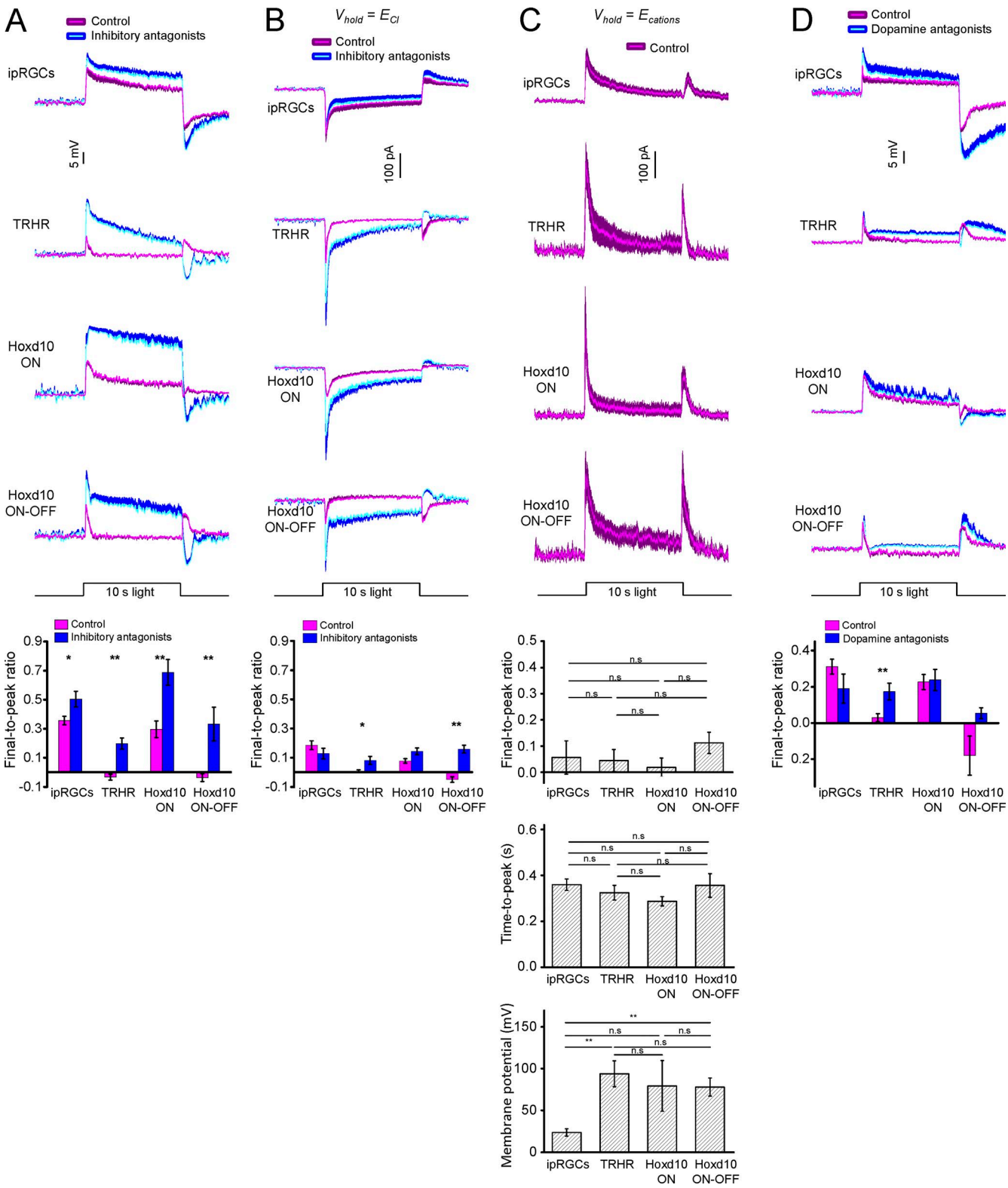

Figure 5. **Regulation by amacrine cells.** (A) Inhibition makes all RGC groups' light-evoked depolarization more transient. (top) Averaged light responses recorded in the presence of normal Ames (magenta traces) and after the addition of 200 µM picrotoxin, 5 µM 3-[[(3,4-dichlorophenyl)methyl]amino]propyl] diethoxymethyl)phosphinic acid (CGP 52432), 30 µM TPMPA, and 10 µM strychnine (blue traces). (bottom) Final-to-peak photoresponse ratios. *n* values: ipRGCs = 10; TRHR = 7; Hoxd10 ON = 8; Hoxd10 ON-OFF = 8. (B) Amacrine inhibition of presynaptic bipolar cells makes some conventional RGCs more transient. Voltage-clamp recordings were made at E_{Cl} to isolate bipolar-cell input. (top) Averaged light responses recorded in the presence of normal Ames (magenta traces) and after the addition of picrotoxin, CGP 52432, TPMPA, and strychnine (blue traces). (bottom) Final-to-peak ratios. *n* values:

smaller (Fig. 6 A, top) and less tonic (Fig. 6 A, bottom). Although it is unclear how the drugs could exert these effects on ipRGCs, we can conclude that AMPA/kainate desensitization does not increase the transience of conventional RGCs' light responses.

We next tested the hypothesis that NMDA receptors contribute to ipRGCs' tonic light responses by recording from some M4 ipRGCs using the normal K^+-based internal solution and from other M4 ipRGCs using the same solution supplemented with 1 mM MK-801, an NMDA receptor antagonist. Resting potentials were unchanged in the presence of MK-801 ($P > 0.05$), and the light responses of the M4 ipRGCs with and without MK-801 had statistically similar final-to-peak ratios (Fig. 6 B, bottom). Though 1 mM intracellular MK-801 should have fully blocked NMDA receptors in RGCs (Manookin et al., 2010), to rule out the possibility that it did not, we also genetically knocked out NMDA receptors selectively in ipRGCs by creating $Opn4^{Cre/+}$; fNR1 mice. Verifying that this knockout was specific to ipRGCs, puffed NMDA evoked robust responses in conventional RGCs (Fig. 6 C, top) but no response in M4 ipRGCs (Fig. 6 C, middle), even though M4 cells normally respond to NMDA in wild-type mice (Fig. 6 C, bottom). Wild-type and $Opn4^{Cre/+}$; fNR1 M4 cells showed similar light responses (Fig. 6 D), confirming that NMDA receptors do not add to the tonic kinetics of M4 cells' rod/cone-mediated light responses.

Glutamate release and uptake

The final experiments investigated mechanisms regulating glutamate release from bipolar cells and glutamate clearance. mGluR7 is present on the axon terminals of some ON and OFF cone bipolar cells and has been proposed to provide a feedback mechanism that regulates glutamate release (Brandstätter et al., 1996). If mGluR7 suppresses glutamate release, it may be expected to make postsynaptic RGCs' light responses more transient, but if it increases glutamate release, it might prolong RGC photoresponses. We tested these possibilities by measuring light responses from RGCs first during normal Ames superfusion and again after applying the mGluR7 antagonist MMPIP. This treatment caused the light responses of ipRGCs and Hoxd10+ ON cells to become significantly more transient, suggesting mGluR7 mediates a positive feedback, while having little effect on TRHR+ or Hoxd10+ ON-OFF RGCs (Fig. 7 A).

After glutamate is released from bipolar cells, it is removed from the synapse by glutamate transporters, thereby terminating glutamatergic excitation of postsynaptic RGCs. To test the hypothesis that this removal contributes to conventional RGCs' transient light responses, we measured light responses first during normal Ames superfusion and then in the presence of the glutamate transporter blocker DL-threo-β-benzyloxyaspartic acid (TBOA). Because the blockade of glutamate transporters is expected to enhance glutamatergic excitation of amacrine cells and hence amacrine-driven inhibition of RGCs, TBOA should ideally be applied after blocking GABA/glycine receptors so that its direct impact on the RGCs can be isolated. But RGCs died quickly when TBOA was applied on top of GABA/glycine receptor antagonists, prompting us to apply TBOA alone. Although the light responses of Hoxd10+ ON cells became smaller (Fig. 7 B, top), final-to-peak ratios were not affected in any of the conventional RGCs (Fig. 7 B, bottom). Surprisingly, TBOA not only made ipRGCs' light responses much smaller (Fig. 7 B, top) but also significantly less tonic (Fig. 7 B, bottom). Although it is unclear how TBOA could make ipRGCs more transient, we can conclude that glutamate uptake does not underlie conventional RGCs' transient light responses.

DISCUSSION

We have investigated what strategies are used by several types of genetically identified RGCs to generate tonic versus transient light responses. A key insight from this work is that different RGC types use diverse strategies to produce transient or tonic light responses, as summarized in Table 2. Thus, some of the candidate mechanisms we refuted could be used by cell types we did not investigate. This finding further suggests that some of the discrepancies in the literature (discussed in the Introduction) could have arisen because different papers sampled from different RGC types, motivating us to reexamine previously tested mechanisms in specific cell types. Another potential cause of discrepancies is that previous studies used diverse metrics to quantify response transience. Indeed, our conclusions regarding some of the 12 candidate mechanisms could have been different had we measured photoresponse sustained-

ipRGCs = 13; TRHR = 5; Hoxd10 ON = 6; Hoxd10 ON-OFF = 6. (C) Comparing amacrine cell–mediated light responses among the RGC groups. Voltage-clamp recordings were made at $E_{cations}$ to isolate Cl^--mediated input. (top) Averaged recordings. (middle top) Final-to-peak ratios. (middle bottom) Times to peak of the ON light responses. (bottom) The impact of the amacrine-driven photocurrents on membrane potential, estimated using Ohm's law (ΔV = photocurrent × membrane resistance). *n* values: ipRGCs = 12; TRHR = 7; Hoxd10 ON = 5; Hoxd10 = 6. (D) Endogenous dopamine makes TRHR+ RGCs more transient. (top) Averaged light responses recorded during superfusion with normal Ames (magenta traces) and in the presence of 60 nM SCH 23390 and 60 nM spiperone (blue traces). (bottom) Final-to-peak ratios. *n* values: ipRGCs = 8; TRHR = 6; Hoxd10 ON = 6; Hoxd10 ON-OFF = 7. All stimuli were the center spot. Error values are SEM. *, $P < 0.05$; **, $P < 0.01$.

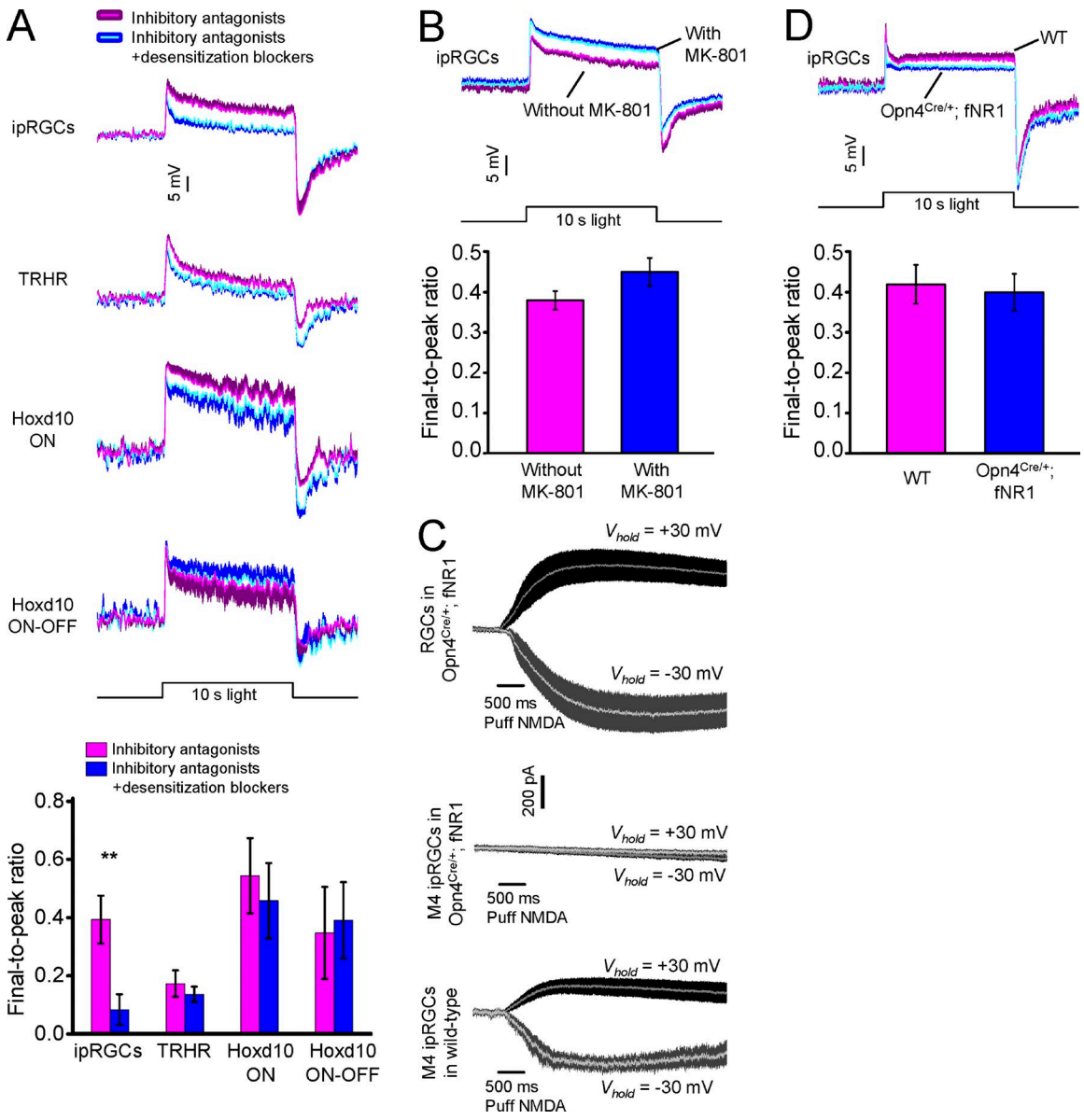

Figure 6. **Examining the dependence of RGC photoresponse kinetics on ionotropic glutamate receptors.** (A) AMPA/kainate receptor desensitization does not make conventional RGCs more transient. (top) Averaged recordings made in the presence of picrotoxin, CGP 52432, TPMPA, and strychnine (magenta traces) and after the addition of 60 µM cyclothiazide and 300 µg/ml concanavalin A (blue traces). (bottom) Final-to-peak ratios. *n* values: ipRGCs = 9; TRHR = 10; Hoxd10 ON = 7; Hoxd10 ON-OFF = 5. (B–D) NMDA receptors do not affect the kinetics of ipRGCs' light responses. (B, top) Averaged light responses recorded without and with intracellular MK-801. (B, bottom) Final-to-peak ratios. *n* values: without MK-801 = 37; with MK-801 = 26. (C, top) In Opn4$^{Cre/+}$; fNR1 mice, NMDA receptors were eliminated selectively in ipRGCs. All conventional RGCs (*n* = 5) in these mice responded to puffed NMDA, whether they were voltage clamped at 30 mV or −30 mV. (C, middle) M4 ipRGCs (*n* = 2) in these knockout mice failed to respond to NMDA at either holding potential. (C, bottom) M4 ipRGCs (*n* = 3) in wild-type mice gave robust NMDA responses. (D, top) Averaged light responses recorded from wild-type and Opn4$^{Cre/+}$; fNR1 M4 ipRGCs. (D, bottom) Final-to-peak ratios. *n* values: wild-type ipRGCs = 9; Opn4$^{Cre/+}$; fNR1 ipRGCs = 9. All stimuli were the center spot. Error values are SEM. **, $P < 0.01$.

ness at a different time point, e.g., 1 s after light onset. We decided to use the final-to-peak response ratio so as to identify mechanisms having relatively pronounced effects on response kinetics.

Center/surround antagonism

We previously reported that among ON and ON-OFF RGCs, only ipRGCs could increase spiking throughout the duration of 10–15-s full-field light (Wong et al., 2007; Wong, 2012). Here, we confirmed that conventional RGCs depolarize very transiently to full-field light, but we found Hoxd10+ ON cells' center responses to be remarkably tonic. Though it may seem logical that an antagonistic surround would enhance the transience of a full-field response, a prior study reported the opposite, with ON RGCs responding more tonically to larger

Table 2. **Mechanisms increasing ipRGCs' or reducing conventional RGCs' final-to-peak photoresponse ratios**

Mechanism	ipRGCs	TRHR+ RGCs	Hoxd10+ ON RGCs	Hoxd10+ ON-OFF RGCs
Center/surround antagonism			X	
Spike frequency adaptation				
Regulation of spiking by resting potential	X		X	
Intracellular Ca^{2+}				
Melanopsin		Not tested	Not tested	Not tested
Tonic versus transient bipolar input	X	X	X	X
Presence or absence of presynaptic inhibition	X	X		X
Dopaminergic modulation		X		
AMPA/kainate receptor desensitization				
NMDA receptors		Not tested	Not tested	Not tested
mGluR7 on presynaptic bipolar cell terminals	X			
Glutamate uptake by transporters				

rather than smaller light spots (Sagdullaev and McCall, 2005). Another study also found that under scotopic conditions, sustained RGCs had receptive field surrounds whereas transient RGCs did not (Hammond, 1975). Thus, what we observed for Hoxd10+ ON cells may be uncommon among RGCs, although it has been reported that many amacrine cells' sustained photoresponses became more phasic as stimulus size increased (Taylor, 1996). In contrast, TRHR+ RGCs and M2–M5 ipRGCs responded more or less equally tonically to the center-selective and full-field stimuli, even though they exhibit pronounced center/surround antagonism. Together, these results indicate that the presence of an antagonistic surround does not necessarily cause a cell to respond more transiently to full-field light. For instance, if the surround response follows the same time course as the center response, surround antagonism might reduce the center response at all time points so that the overall photoresponse waveform is unaffected. However, an important caveat is that we tested only one

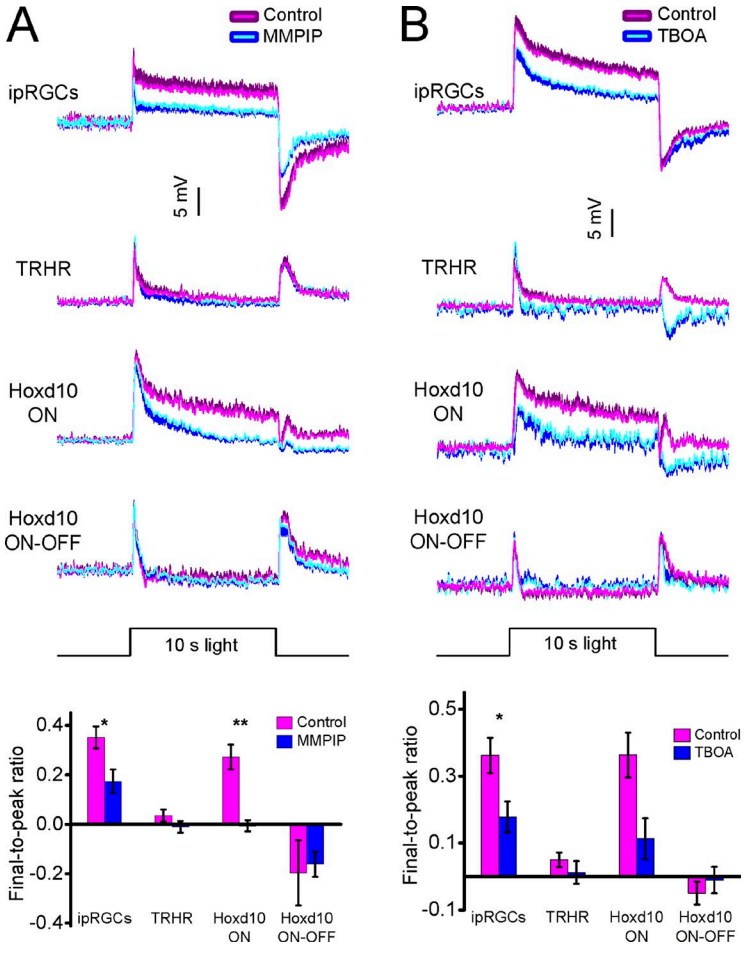

Figure 7. **Examining the dependence of RGC photoresponse kinetics on mechanisms regulating glutamate release or reuptake.** (A) mGluR7 makes two RGC groups more tonic. (top) Averaged light responses recorded during superfusion with normal Ames (magenta traces) and after the addition of 10 µM MMPIP (blue traces). (bottom) Final-to-peak ratios. *n* values: ipRGCs = 8; TRHR = 7; Hoxd10 ON = 6; Hoxd10 ON-OFF = 7. (B, top) Averaged light responses recorded during superfusion with normal Ames (magenta traces) and after the addition of 25 µM TBOA (blue traces). (bottom) Final-to-peak ratios. *n* values: ipRGCs = 10; TRHR = 8; Hoxd10 ON = 6; Hoxd10 ON-OFF = 6. All stimuli were the center spot. Error values are SEM. *, $P < 0.05$; **, $P < 0.01$.

spot diameter (200 µm), which probably did not equally stimulate the various RGC types' center regions. It remains possible that some other spot diameters would have revealed a role for center/surround antagonism in shaping photoresponse transience in RGCs other than the Hoxd10+ ON cells.

Intrinsic mechanisms

Recording from salamander RGCs, Mobbs et al. (Mobbs et al., 1992) found that depolarizing current steps evoked tonic spiking in cells displaying tonic photoresponses but transient spiking in cells that responded transiently to light. Tonic versus phasic current-induced spiking responses have also been observed among goldfish RGCs (Tabata and Kano, 2002). In contrast, all types of cat RGCs exhibited similar amounts of spike rate adaptation during current injection (O'Brien et al., 2002), mirroring what we observed in the present study. However, another study by O'Brien et al. reported a substantially wider range of spike rate adaptation among rat RGCs (Wong et al., 2012). Thus, spike rate adaptation may play a more important role in diversifying RGC physiology in some species than in others.

Our previous studies of extraordinarily high spontaneous spike rates in ipRGCs in mice (Zhao et al., 2014) and rats (Reifler et al., 2015) were puzzling because spike generation is metabolically costly (Perge et al., 2009). Results from the present study suggest that having an unusually positive resting membrane potential (and hence high spontaneous spiking activity) helps ipRGCs produce tonic spiking during prolonged illumination, whereas the far more negative resting potential in Hoxd10+ ON cells appears to increase the transience of their spiking photoresponses. Interestingly, it has been reported that mouse RGCs that responded tonically to light had spontaneous spiking, whereas those with phasic light responses did not (Ekesten and Gouras, 2005).

In some neurons, a synaptically driven rise in intracellular Ca^{2+} exerts a negative feedback that reduces the amplitude of the synaptic input; for instance, intracellular Ca^{2+} has been shown to suppress excitatory light responses in RGCs (Akopian and Witkovsky, 2001). This feedback could conceivably make a light response more phasic, and we wondered whether chelating intracellular Ca^{2+} would increase the sustainedness of conventional RGCs. Though the light responses of ipRGCs and Hoxd10+ ON cells became larger, possibly reflecting the removal of Ca^{2+}-mediated inhibition, we did not detect a significant change in photoresponse transience.

ipRGCs generate impressively long-lasting intrinsic and rod/cone-driven light responses. Though several mechanisms enabling the tonic kinetics of the intrinsic response are known (Emanuel and Do, 2015; Mure et al., 2016; Zhao et al., 2016), mechanisms for sustained rod/cone input are less understood. We previously showed that melanopsin-knockout ipRGCs could still respond continuously to 20-min light, indicating melanopsin is not required, but we did not quantify whether eliminating melanopsin reduced photoresponse sustainedness to some degree (Wong, 2012). In the current study, we found that responses to rod/cone-selective 10-s light were unaffected.

The role of mGluR6 in determining photoresponse kinetics

As mentioned earlier, Kaur and Nawy (2012) challenged the findings of Awatramani and Slaughter (2000) by showing that mGluR antagonist-induced excitations of transient and sustained ON bipolar cells decayed with similar kinetics. We propose the following to reconcile these studies. Kaur and Nawy (2012) did not measure light responses but instead assumed ON bipolar cells with axons terminating near the middle of the inner plexiform layer to be transient and those terminating more proximally to be sustained (Vallerga and Usai, 1986). However, a larger-scale study has found no correlation between salamander bipolar cells' photoresponse kinetics and axonal stratification levels (Pang et al., 2004). As shown in Fig. 4 A of Kaur and Nawy (2012), the decay rates of the antagonist-induced responses spanned a very wide range. We surmise that the cells that responded to the antagonist transiently would have given transient light responses, whereas those that responded tonically probably had sustained photoresponses.

GABA, glycine, and dopamine

We failed to detect presynaptic amacrine-to-bipolar inhibition for ipRGCs, consistent with electron microscopy evidence that ON bipolar cells usually form one-to-one synapses with ipRGCs (Kim et al., 2012) rather than the far more common arrangement, where the bipolar cell signals to one RGC and one amacrine cell, which allows for amacrine-to-bipolar inhibition (Dowling, 1968). The lack of presynaptic amacrine-to-bipolar inhibition may explain why antagonizing GABAergic/glycinergic inhibition seemed to affect ipRGCs less than the other RGC types (Fig. 5 A, bottom). Though Hoxd10+ ON cells do experience amacrine-to-bipolar inhibition (Fig. 5 B, top), it does not significantly affect these cells' photoresponse transience (Fig. 5 B, bottom), which may contribute to their relatively tonic center responses (Fig. 2). Although all RGCs receive substantial amacrine input, this input appears smaller in ipRGCs than in conventional RGCs, which could potentially further enhance ipRGCs' sustainedness.

Dopamine acts as a light-adaptive signal that promotes cone function (Witkovsky, 2004). It is secreted from amacrine cells during subjective daytime (Doyle et al., 2002), and we found that blocking daytime dopaminergic signaling caused TRHR+ RGCs to respond more

tonically to light, suggesting that endogenous dopamine makes them more transient. Such modulation presumably helps these direction-selective cells detect high-frequency visual stimuli under daylight conditions. Though dopamine receptor blockade did not significantly affect the transience of rod/cone-driven ipRGC photoresponses, it made them larger (Fig. 5 D, top), suggesting that dopamine attenuates not only the intrinsic light response of ipRGCs (Van Hook et al., 2012) but also their extrinsic light response.

AMPA/kainate receptor desensitization and NMDA receptors

Although blocking AMPA desensitization had been reported to dramatically potentiate glutamatergic input to RGCs (Lukasiewicz et al., 1995; Matsui et al., 1998), we found such blockade to only slightly increase the ON responses of Hoxd10+ ON-OFF cells while paradoxically attenuating those of the other three RGC groups. The main difference between those studies and ours is that we first blocked GABA/glycine signaling before blocking AMPA/kainate desensitization. It is possible that the prolonged absence of inhibition significantly depleted the pool of releasable vesicles in bipolar terminals by stimulating spontaneous release. In any case, we found no evidence that AMPA/kainate desensitization adds to the transience of conventional RGCs' light responses.

We previously detected functional NMDA receptors on M1 ipRGCs (Wong et al., 2007), and here, we have extended this finding to M4 cells. Eliminating NMDA input had no impact on M4 cells' photoresponses, suggesting these receptors are extrasynaptic (Zhang and Diamond, 2006). However, we only tested a very low light intensity, for only 10 s, to avoid stimulating melanopsin. It remains possible that higher light intensities and/or longer stimulation would activate NMDA receptors and prolong ipRGCs' light responses.

Regulation of glutamate release and reuptake

Group III mGluRs include types 4, 6, 7, and 8. Types 4, 7 and 8 have been detected in the inner plexiform layer, with mGluRs 4 and 7 primarily found in bipolar cell axons (Quraishi et al., 2007). The influence of these receptors on bipolar-to-RGC signaling has been investigated using group III mGluR agonists and antagonists (Awatramani and Slaughter, 2001; Higgs et al., 2002), but these studies could not examine modulation of ON bipolar-driven light responses because these drugs would have blocked such responses by acting on mGluR6. The development of the mGluR7-specific antagonist MMPIP (Suzuki et al., 2007) enabled us to block mGluR7 selectively. In the presence of MMPIP, ipRGCs' and Hoxd10+ ON RGCs' light responses became less tonic (Fig. 7 A, top), suggesting that mGluR7 helps maintain glutamate release during continued illumination. This constitutes positive feedback as opposed to the transporter-mediated negative feedback of glutamate release from bipolar cell terminals (Veruki et al., 2006) and may contribute to the relatively sustained center light responses of ipRGCs and Hoxd10+ ON RGCs (Fig. 2). mGluR7 activation has indeed been shown to increase glutamate release in the inner plexiform layer (Guimarães-Souza and Calaza, 2012).

Contrary to the previous demonstration that blocking glutamate uptake enhanced bipolar input to RGCs (Higgs and Lukasiewicz, 1999), we found that most RGCs' ON photoresponses became smaller, especially ipRGCs'. A possible explanation is that bipolar input was isolated under voltage clamp in that previous study, whereas our current-clamp recordings permitted both bipolar and amacrine inputs. TBOA likely increased glutamatergic activation of amacrine cells, which in turn inhibited RGCs. We had tried to first block GABA/glycine signaling, but the subsequent addition of TBOA invariably caused rapid cell death. Nonetheless, this experiment's aim was to investigate mechanisms producing conventional RGCs' transient photoresponses, and TBOA's insignificant effects ruled out glutamate uptake as a contributing mechanism.

Summary

We have explored 12 mechanisms hypothesized to shape photoresponse kinetics in mouse RGCs. In addition to confirming or refuting several previously proposed mechanisms, our results implicated the involvement of three novel mechanisms: center/surround antagonism, adjustment of resting potentials, and mGluR7. Another new finding, made possible by our testing all 12 candidate mechanisms in every RGC type, is that each type uses a unique combination of mechanisms to control photoresponse kinetics. Future work will be needed to characterize the new mechanisms in further detail, address the relative importance and different roles of the two to four mechanisms used by each RGC, and test additional potential mechanisms, such as synaptic depression, photoreceptor adaptation, and the many neuromodulators besides dopamine.

ACKNOWLEDGMENTS

We thank Marla Feller for the TRHR-GFP mice, David Berson for the Hoxd10-GFP mice, and Samer Hattar for the $Opn4^{Cre/Cre}$ mice.

This work was funded by National Eye Institute grants R01 EY023660 (to K.Y. Wong) and P30 EY007003 (Vision Research Core Grant).

The authors declare no competing financial interests.

Author contributions: K.Y. Wong designed the research. X. Zhao, A.N. Reifler, M.M. Schroeder, and E.R. Jaeckel performed experiments. A.P. Chervenak and K.Y. Wong provided technical support. X. Zhao and A.N. Reifler analyzed the data. K.Y. Wong wrote the manuscript.

Richard W. Aldrich served as editor.

Submitted: 1 November 2016
Accepted: 30 December 2016

REFERENCES

Akopian, A., and P. Witkovsky. 2001. Intracellular calcium reduces light-induced excitatory post-synaptic responses in salamander retinal ganglion cells. *J. Physiol.* 532:43–53. http://dx.doi.org/10.1111/j.1469-7793.2001.0043g.x

Awatramani, G.B., and M.M. Slaughter. 2000. Origin of transient and sustained responses in ganglion cells of the retina. *J. Neurosci.* 20:7087–7095.

Awatramani, G.B., and M.M. Slaughter. 2001. Intensity-dependent, rapid activation of presynaptic metabotropic glutamate receptors at a central synapse. *J. Neurosci.* 21:741–749.

Baden, T., P. Berens, K. Franke, M. Román Rosón, M. Bethge, and T. Euler. 2016. The functional diversity of retinal ganglion cells in the mouse. *Nature.* 529:345–350. http://dx.doi.org/10.1038/nature16468

Berntson, A., R.G. Smith, and W.R. Taylor. 2004. Postsynaptic calcium feedback between rods and rod bipolar cells in the mouse retina. *Vis. Neurosci.* 21:913–924. http://dx.doi.org/10.1017/S095252380421611X

Bieda, M.C., and D.R. Copenhagen. 2000. Inhibition is not required for the production of transient spiking responses from retinal ganglion cells. *Vis. Neurosci.* 17:243–254. http://dx.doi.org/10.1017/S0952523800172062

Bonaventure, N., N. Wioland, and G. Roussel. 1980. Effects of some amino acids (GABA, glycine, taurine) and of their antagonists (picrotoxin, strychnine) on spatial and temporal features of frog retinal ganglion cell responses. *Pflugers Arch.* 385:51–64. http://dx.doi.org/10.1007/BF00583915

Brandstätter, J.H., P. Koulen, R. Kuhn, H. van der Putten, and H. Wässle. 1996. Compartmental localization of a metabotropic glutamate receptor (mGluR7): two different active sites at a retinal synapse. *J. Neurosci.* 16:4749–4756.

Brecha, N.C. 2004. Peptide and peptide receptor expression and function in the vertebrate retina. *In* The Visual Neurosciences. L.M. Chalupa, and J.S. Werner, editors. MIT Press, Cambridge, MA. 334–354.

Caldwell, J.H., and N.W. Daw. 1978. New properties of rabbit retinal ganglion cells. *J. Physiol.* 276:257–276. http://dx.doi.org/10.1113/jphysiol.1978.sp012232

Cleland, B.G., M.W. Dubin, and W.R. Levick. 1971. Sustained and transient neurones in the cat's retina and lateral geniculate nucleus. *J. Physiol.* 217:473–496. http://dx.doi.org/10.1113/jphysiol.1971.sp009581

Copenhagen, D.R., and C.E. Jahr. 1989. Release of endogenous excitatory amino acids from turtle photoreceptors. *Nature.* 341:536–539. http://dx.doi.org/10.1038/341536a0

Dhande, O.S., M.E. Estevez, L.E. Quattrochi, R.N. El-Danaf, P.L. Nguyen, D.M. Berson, and A.D. Huberman. 2013. Genetic dissection of retinal inputs to brainstem nuclei controlling image stabilization. *J. Neurosci.* 33:17797–17813. http://dx.doi.org/10.1523/JNEUROSCI.2778-13.2013

Diamond, J.S., and D.R. Copenhagen. 1993. The contribution of NMDA and non-NMDA receptors to the light-evoked input-output characteristics of retinal ganglion cells. *Neuron.* 11:725–738. http://dx.doi.org/10.1016/0896-6273(93)90082-3

Dowling, J.E. 1968. Synaptic organization of the frog retina: an electron microscopic analysis comparing the retinas of frogs and primates. *Proc. R. Soc. Lond. B Biol. Sci.* 170:205–228. http://dx.doi.org/10.1098/rspb.1968.0034

Dowling, J.E., and H. Ripps. 1973. Effect of magnesium on horizontal cell activity in the skate retina. *Nature.* 242:101–103. http://dx.doi.org/10.1038/242101a0

Doyle, S.E., W.E. McIvor, and M. Menaker. 2002. Circadian rhythmicity in dopamine content of mammalian retina: Role of the photoreceptors. *J. Neurochem.* 83:211–219. http://dx.doi.org/10.1046/j.1471-4159.2002.01149.x

Ecker, J.L., O.N. Dumitrescu, K.Y. Wong, N.M. Alam, S.K. Chen, T. LeGates, J.M. Renna, G.T. Prusky, D.M. Berson, and S. Hattar. 2010. Melanopsin-expressing retinal ganglion-cell photoreceptors: Cellular diversity and role in pattern vision. *Neuron.* 67:49–60. http://dx.doi.org/10.1016/j.neuron.2010.05.023

Ekesten, B., and P. Gouras. 2005. Cone and rod inputs to murine retinal ganglion cells: evidence of cone opsin specific channels. *Vis. Neurosci.* 22:893–903. http://dx.doi.org/10.1017/S0952523805226172

Emanuel, A.J., and M.T. Do. 2015. Melanopsin tristability for sustained and broadband phototransduction. *Neuron.* 85:1043–1055. http://dx.doi.org/10.1016/j.neuron.2015.02.011

Estevez, M.E., P.M. Fogerson, M.C. Ilardi, B.G. Borghuis, E. Chan, S. Weng, O.N. Auferkorte, J.B. Demb, and D.M. Berson. 2012. Form and function of the M4 cell, an intrinsically photosensitive retinal ganglion cell type contributing to geniculocortical vision. *J. Neurosci.* 32:13608–13620. http://dx.doi.org/10.1523/JNEUROSCI.1422-12.2012

Frumkes, T.E., R. Nelson, and R. Pflug. 1995. Functional role of GABA in cat retina: II. Effects of GABAA antagonists. *Vis. Neurosci.* 12:651–661. http://dx.doi.org/10.1017/S0952523800008944

Gouras, P. 1968. Identification of cone mechanisms in monkey ganglion cells. *J. Physiol.* 199:533–547. http://dx.doi.org/10.1113/jphysiol.1968.sp008667

Granda, A.M., and J.E. Fulbrook. 1989. Classification of turtle retinal ganglion cells. *J. Neurophysiol.* 62:723–737.

Guimarães-Souza, E.M., and K.C. Calaza. 2012. Selective activation of group III metabotropic glutamate receptor subtypes produces different patterns of γ-aminobutyric acid immunoreactivity and glutamate release in the retina. *J. Neurosci. Res.* 90:2349–2361. http://dx.doi.org/10.1002/jnr.23123

Hammond, P. 1975. Receptive field mechanisms of sustained and transient retinal ganglion cells in the cat. *Exp. Brain Res.* 23:113–128. http://dx.doi.org/10.1007/BF00235454

Higgs, M.H., and P.D. Lukasiewicz. 1999. Glutamate uptake limits synaptic excitation of retinal ganglion cells. *J. Neurosci.* 19:3691–3700.

Higgs, M.H., C. Romano, and P.D. Lukasiewicz. 2002. Presynaptic effects of group III metabotropic glutamate receptors on excitatory synaptic transmission in the retina. *Neuroscience.* 115:163–172. http://dx.doi.org/10.1016/S0306-4522(02)00381-0

Hu, C., D.D. Hill, and K.Y. Wong. 2013. Intrinsic physiological properties of the five types of mouse ganglion-cell photoreceptors. *J. Neurophysiol.* 109:1876–1889. http://dx.doi.org/10.1152/jn.00579.2012

Ikeda, H., and M.J. Sheardown. 1982. Aspartate may be an excitatory transmitter mediating visual excitation of "sustained" but not "transient" cells in the cat retina: Iontophoretic studies in vivo. *Neuroscience.* 7:25–36. http://dx.doi.org/10.1016/0306-4522(82)90150-6

Jensen, R.J., and N.W. Daw. 1984. Effects of dopamine antagonists on receptive fields of brisk cells and directionally selective cells in the rabbit retina. *J. Neurosci.* 4:2972–2985.

Jones, I.L., T.L. Russell, K. Farrow, M. Fiscella, F. Franke, J. Müller, D. Jäckel, and A. Hierlemann. 2015. A method for electrophysiological characterization of hamster retinal ganglion

cells using a high-density CMOS microelectrode array. *Front. Neurosci.* 9:360. http://dx.doi.org/10.3389/fnins.2015.00360

Kaneko, A. 1970. Physiological and morphological identification of horizontal, bipolar and amacrine cells in goldfish retina. *J. Physiol.* 207:623–633. http://dx.doi.org/10.1113/jphysiol.1970.sp009084

Kaur, T., and S. Nawy. 2012. Characterization of Trpm1 desensitization in ON bipolar cells and its role in downstream signalling. *J. Physiol.* 590:179–192. http://dx.doi.org/10.1113/jphysiol.2011.218974

Kim, H.L., J.H. Jeon, T.H. Koo, U.Y. Lee, E. Jeong, M.H. Chun, J.I. Moon, S.C. Massey, and I.B. Kim. 2012. Axonal synapses utilize multiple synaptic ribbons in the mammalian retina. *PLoS One.* 7:e52295. http://dx.doi.org/10.1371/journal.pone.0052295

Lu, H.D., and H.M. Petry. 2003. Temporal modulation sensitivity of tree shrew retinal ganglion cells. *Vis. Neurosci.* 20:363–372. http://dx.doi.org/10.1017/S0952523803204028

Lukasiewicz, P.D., J.E. Lawrence, and T.L. Valentino. 1995. Desensitizing glutamate receptors shape excitatory synaptic inputs to tiger salamander retinal ganglion cells. *J. Neurosci.* 15:6189–6199.

Maguire, G. 1999. Rapid desensitization converts prolonged glutamate release into a transient EPSC at ribbon synapses between retinal bipolar and amacrine cells. *Eur. J. Neurosci.* 11:353–362. http://dx.doi.org/10.1046/j.1460-9568.1999.00439.x

Maguire, G.W., and E.L. Smith III. 1985. Cat retinal ganglion cell receptive-field alterations after 6-hydroxydopamine induced dopaminergic amacrine cell lesions. *J. Neurophysiol.* 53:1431–1443.

Manookin, M.B., M. Weick, B.K. Stafford, and J.B. Demb. 2010. NMDA receptor contributions to visual contrast coding. *Neuron.* 67:280–293. http://dx.doi.org/10.1016/j.neuron.2010.06.020

Masland, R.H. 2012. The tasks of amacrine cells. *Vis. Neurosci.* 29:3–9. http://dx.doi.org/10.1017/S0952523811000344

Masu, M., H. Iwakabe, Y. Tagawa, T. Miyoshi, M. Yamashita, Y. Fukuda, H. Sasaki, K. Hiroi, Y. Nakamura, R. Shigemoto, et al. 1995. Specific deficit of the ON response in visual transmission by targeted disruption of the mGluR6 gene. *Cell.* 80:757–765. http://dx.doi.org/10.1016/0092-8674(95)90354-2

Matsui, K., N. Hosoi, and M. Tachibana. 1998. Excitatory synaptic transmission in the inner retina: Paired recordings of bipolar cells and neurons of the ganglion cell layer. *J. Neurosci.* 18:4500–4510.

Matsui, K., N. Hosoi, and M. Tachibana. 1999. Active role of glutamate uptake in the synaptic transmission from retinal nonspiking neurons. *J. Neurosci.* 19:6755–6766.

Mobbs, P., K. Everett, and A. Cook. 1992. Signal shaping by voltage-gated currents in retinal ganglion cells. *Brain Res.* 574:217–223. http://dx.doi.org/10.1016/0006-8993(92)90819-U

Mure, L.S., M. Hatori, Q. Zhu, J. Demas, I.M. Kim, S.K. Nayak, and S. Panda. 2016. Melanopsin-encoded response properties of intrinsically photosensitive retinal ganglion cells. *Neuron.* 90:1016–1027. http://dx.doi.org/10.1016/j.neuron.2016.04.016

Nirenberg, S., and M. Meister. 1997. The light response of retinal ganglion cells is truncated by a displaced amacrine circuit. *Neuron.* 18:637–650. http://dx.doi.org/10.1016/S0896-6273(00)80304-9

O'Brien, B.J., T. Isayama, R. Richardson, and D.M. Berson. 2002. Intrinsic physiological properties of cat retinal ganglion cells. *J. Physiol.* 538:787–802. http://dx.doi.org/10.1113/jphysiol.2001.013009

Pang, J.J., F. Gao, and S.M. Wu. 2004. Stratum-by-stratum projection of light response attributes by retinal bipolar cells of Ambystoma. *J. Physiol.* 558:249–262. http://dx.doi.org/10.1113/jphysiol.2004.063503

Pang, J.J., F. Gao, A. Barrow, R.A. Jacoby, and S.M. Wu. 2008. How do tonic glutamatergic synapses evade receptor desensitization? *J. Physiol.* 586:2889–2902. http://dx.doi.org/10.1113/jphysiol.2008.151050

Perge, J.A., K. Koch, R. Miller, P. Sterling, and V. Balasubramanian. 2009. How the optic nerve allocates space, energy capacity, and information. *J. Neurosci.* 29:7917–7928. http://dx.doi.org/10.1523/JNEUROSCI.5200-08.2009

Popova, E., L. Mitova, L. Vitanova, and P. Kupenova. 2003. Effect of GABAergic blockade on light responses of frog retinal ganglion cells. *Comp. Biochem. Physiol. C Toxicol. Pharmacol.* 134:175–187. http://dx.doi.org/10.1016/S1532-0456(02)00246-6

Quraishi, S., J. Gayet, C.W. Morgans, and R.M. Duvoisin. 2007. Distribution of group-III metabotropic glutamate receptors in the retina. *J. Comp. Neurol.* 501:931–943. http://dx.doi.org/10.1002/cne.21274

Reifler, A.N., A.P. Chervenak, M.E. Dolikian, B.A. Benenati, B.S. Meyers, Z.D. Demertzis, A.M. Lynch, B.Y. Li, R.D. Wachter, F.S. Abufarha, et al. 2015. The rat retina has five types of ganglion-cell photoreceptors. *Exp. Eye Res.* 130:17–28. http://dx.doi.org/10.1016/j.exer.2014.11.010

Rivlin-Etzion, M., K. Zhou, W. Wei, J. Elstrott, P.L. Nguyen, B.A. Barres, A.D. Huberman, and M.B. Feller. 2011. Transgenic mice reveal unexpected diversity of on-off direction-selective retinal ganglion cell subtypes and brain structures involved in motion processing. *J. Neurosci.* 31:8760–8769. http://dx.doi.org/10.1523/JNEUROSCI.0564-11.2011

Sagdullaev, B.T., and M.A. McCall. 2005. Stimulus size and intensity alter fundamental receptive-field properties of mouse retinal ganglion cells in vivo. *Vis. Neurosci.* 22:649–659. http://dx.doi.org/10.1017/S0952523805225142

Schmidt, T.M., and P. Kofuji. 2011. Structure and function of bistratified intrinsically photosensitive retinal ganglion cells in the mouse. *J. Comp. Neurol.* 519:1492–1504. http://dx.doi.org/10.1002/cne.22579

Sethuramanujam, S., and M.M. Slaughter. 2015. Properties of a glutamatergic synapse controlling information output from retinal bipolar cells. *PLoS One.* 10:e0129133. http://dx.doi.org/10.1371/journal.pone.0129133

Slaughter, M.M., and R.F. Miller. 1981. 2-amino-4-phosphonobutyric acid: a new pharmacological tool for retina research. *Science.* 211:182–185. http://dx.doi.org/10.1126/science.6255566

Slaughter, M.M., and R.F. Miller. 1983. The role of excitatory amino acid transmitters in the mudpuppy retina: an analysis with kainic acid and N-methyl aspartate. *J. Neurosci.* 3:1701–1711.

Suzuki, G., N. Tsukamoto, H. Fushiki, A. Kawagishi, M. Nakamura, H. Kurihara, M. Mitsuya, M. Ohkubo, and H. Ohta. 2007. In vitro pharmacological characterization of novel isoxazolopyridone derivatives as allosteric metabotropic glutamate receptor 7 antagonists. *J. Pharmacol. Exp. Ther.* 323:147–156. http://dx.doi.org/10.1124/jpet.107.124701

Tabata, T., and M. Kano. 2002. Heterogeneous intrinsic firing properties of vertebrate retinal ganglion cells. *J. Neurophysiol.* 87:30–41.

Taylor, W.R. 1996. Response properties of long-range axon-bearing amacrine cells in the dark-adapted rabbit retina. *Vis. Neurosci.* 13:599–604. http://dx.doi.org/10.1017/S0952523800008506

Tran, M.N., M.H. Higgs, and P.D. Lukasiewicz. 1999. AMPA receptor kinetics limit retinal amacrine cell excitatory synaptic responses. *Vis. Neurosci.* 16:835–842. http://dx.doi.org/10.1017/S0952523899165039

Tsien, J.Z., P.T. Huerta, and S. Tonegawa. 1996. The essential role of hippocampal CA1 NMDA receptor-dependent synaptic plasticity in spatial memory. *Cell.* 87:1327–1338. http://dx.doi.org/10.1016/S0092-8674(00)81827-9

Vallerga, S., and C. Usai. 1986. Relation between light responses and dendritic branching in the salamander ganglion cells. *Exp. Biol.* 45:81–90.

Van Hook, M.J., K.Y. Wong, and D.M. Berson. 2012. Dopaminergic modulation of ganglion-cell photoreceptors in rat. *Eur. J. Neurosci.* 35:507–518. http://dx.doi.org/10.1111/j.1460-9568.2011.07975.x

Vaquero, C.F., A. Pignatelli, G.J. Partida, and A.T. Ishida. 2001. A dopamine- and protein kinase A-dependent mechanism for network adaptation in retinal ganglion cells. *J. Neurosci.* 21:8624–8635.

Veruki, M.L., S.H. Mørkve, and E. Hartveit. 2006. Activation of a presynaptic glutamate transporter regulates synaptic transmission through electrical signaling. *Nat. Neurosci.* 9:1388–1396. http://dx.doi.org/10.1038/nn1793

Werblin, F.S., and J.E. Dowling. 1969. Organization of the retina of the mudpuppy, *Necturus maculosus*. II. Intracellular recording. *J. Neurophysiol.* 32:339–355.

Witkovsky, P. 2004. Dopamine and retinal function. *Doc. Ophthalmol.* 108:17–39. http://dx.doi.org/10.1023/B:DOOP.0000019487.88486.0a

Wong, K.Y. 2012. A retinal ganglion cell that can signal irradiance continuously for 10 hours. *J. Neurosci.* 32:11478–11485. http://dx.doi.org/10.1523/JNEUROSCI.1423-12.2012

Wong, K.Y., F.A. Dunn, D.M. Graham, and D.M. Berson. 2007. Synaptic influences on rat ganglion-cell photoreceptors. *J. Physiol.* 582:279–296. http://dx.doi.org/10.1113/jphysiol.2007.133751

Wong, R.C., S.L. Cloherty, M.R. Ibbotson, and B.J. O'Brien. 2012. Intrinsic physiological properties of rat retinal ganglion cells with a comparative analysis. *J. Neurophysiol.* 108:2008–2023. http://dx.doi.org/10.1152/jn.01091.2011

Zhang, C., and M.A. McCall. 2012. Receptor targets of amacrine cells. *Vis. Neurosci.* 29:11–29. http://dx.doi.org/10.1017/S0952523812000028

Zhang, J., and J.S. Diamond. 2006. Distinct perisynaptic and synaptic localization of NMDA and AMPA receptors on ganglion cells in rat retina. *J. Comp. Neurol.* 498:810–820. http://dx.doi.org/10.1002/cne.21089

Zhao, X., B.K. Stafford, A.L. Godin, W.M. King, and K.Y. Wong. 2014. Photoresponse diversity among the five types of intrinsically photosensitive retinal ganglion cells. *J. Physiol.* 592:1619–1636. http://dx.doi.org/10.1113/jphysiol.2013.262782

Zhao, X., W. Pack, N.W. Khan, and K.Y. Wong. 2016. Prolonged inner retinal photoreception depends on the visual retinoid cycle. *J. Neurosci.* 36:4209–4217. http://dx.doi.org/10.1523/JNEUROSCI.2629-14.2016